DISSERTATION

On

"AN EXPERIMENTAL STUDY OF SLOSHING IN WATER TANKS UNDER SEISMIC CONDITION"

Submitted by-
Vipul Kumar Arya
M.Tech (Structural Engineering)

2K14/STE/20

Under the guidance of-
Dr. AlokVerma
Associate Professor
(Department of Civil Engineering)
Delhi Technological University

Department of Civil Engineering
Delhi Technological University (D.T.U.), Delhi-110042
June 2016

CERTIFICATE

I hereby certify that the work which is being presented in the thesis, entitled "**An Experimental study of sloshing in water tanks under seismic condition**" for the award of the degree of Master of Technology submitted in the department of Civil Engineering, Delhi Technological University, Delhi, is an authentic record of my own work carried out under the supervision of Dr.AlokVerma, Associate Professor, Department of Civil Engineering, Delhi Technological University, Delhi, India. The matter presented here in this thesis has not been submitted in part or in full for award of degree/diploma of this or any other University/Institute.

VIPUL KUMAR ARYA

2K14/STE/20

This is to certify that the candidates declaration, above, is correct to the best of the my knowledge and belief.

AlokVerma
Associate Professor
Department of Civil Engineering
Delhi Technological University, Delhi

ACKNOWLEDGEMENT

I am extremely fortunate to be involved in an exciting and challenging research project like "**An Experimental study of sloshing in water tanks under seismic condition**". This project increased my thinking and understanding capability.

I would like to express my greatest gratitude to my supervisor Dr.*AlokVerma (AssociateProfessor, Delhi Technological University)*, for hisexcellent guidance, valuable suggestions and endless support. Dr. Prof N. Dev, Head of Civil Engineering Department, has been a source of inspiration, I thank him for his constant support.

I would like to express my sincere thanks to all my classmatesfor theirprecious suggestions and encouragement to perform the project work. I am very much thankful to them for giving their valuable time to me.

Finally,I express my sincere gratitude to my parents for their constant encouragement and support.

VIPUL KUMAR ARYA

ROLL NO. – 2K14/STE/20

M.TECH

DELHI TECHNOLOGICAL UNIVERSITY

ABSTRACT

Sloshing is defined as the movement of liquid surface inside a tank. For sloshing, it is necessary to have a free surface of liquid. It encompasses a wide spectrum of problems in engineering interests. Study of sloshing phenomenon in water tanks is very vital during the event of earthquake because water tanks play a key role in relief operations after disasters. Thus, securing water for domestic purposes and fire control operations until the restoration of uninterrupted water supply is very important for disaster victims. During earthquakes, additional fluid pressure is exerted on the walls of the water tank. Therefore, a detailed analysis of the water storage tanks during seismic excitations is crucial for safe design of the water tanks.

It is observed that water tanks that were inadequately designed suffered considerable damage in past earthquakes. In this study, a rectangular model of water tank is excited at its natural frequency for various conditions.

The experimental programme included the study of the effect of various parameters on the sloshing behaviour of water inside the tank. Different levels of water inside the tank, location of baffle walls (used to moderate sloshing) inside the tank, type of baffle walls in terms of induced perforations inside them and the extent and placement of perforations of baffle walls where some parameters involved in the study.

Results of the above mentioned parameters on the sloshing of water have been reported in this dissertation report. It is appreciated that study of these parameters may be useful in providing optimum designs of water tanks.

List of Tables

List of Figures

Fig 5.26Comparison between unbaffled tank, tank with 25 cm baffle wall and tank with perforated baffle wall at frequency of 2.8 Hz

Contents

CHAPTER 1

INTRODUCTION

1.1 Introduction

Sloshing is a well known phenomenon in liquid storage tank subjected to seismic loading or body motions. It is defined as movement of free liquid surface in a partially filled liquid tank.Sloshing behaviour of liquids within containers represents one of the most fundamental fluid-structure interactions. The movement of liquid having a free surface is important in various engineering problems like propellant slosh in spacecraft and rockets, cargo slosh in ships and trucks transporting oil or gasoline, water oscillation in a reservoir due to earthquake, sloshing in tanks of boiling water reactors and several others. Containers having liquid with a free surface should be moved with complete care to avoid spilling and other damages. Whenever there is free surface of liquid, oscillations or liquid sloshing will be induced on the container walls. Liquid sloshing problem involves the estimation of pressure distribution in the tank, moments and forces developed by fluid motion, and natural frequencies of the free surfaces of the liquid inside container. These parameters can directly influence the dynamic stability and performance of moving containers. Generally, estimation of hydrodynamic pressure in moving rigid containers has two different components. First one is caused by moving fluid with same tank velocity and is directly proportional to the acceleration of the tank. The second component represents free-surface-liquid motion and known as convective pressure.
Sloshing may result in resonant excitation of the liquid inside tank.

The fluid sloshing in storage tanks when seismically excited can cause severe problems, such as, tanks roof failure, fire of oil-storage tanks. Thus to avoid sloshing movement to impact tank roof, Maximum sloshing wave height is used to provide adequate freeboard for liquid surface. Large amplitude sloshing waves are the main reason for nonlinear slosh effects. These waves emerge when seismic wave frequency coincides with the natural period or resonant frequency of earthquake excited motion for longer periods. When the wave amplitude is large enough to create dynamic effects on fluid container and there is a change the free surface boundary condition, the assumption of linear theory is not valid, thus non-linear effects of liquid should be taken into account and also the moving boundary condition on free surfaces.

Civil Engineers and seismologists have been studying liquid sloshing effects on large dams, oil tanks and elevated water towers under ground motion. Since early 1950s, the problem of liquid sloshing dynamics has been of major concern to aerospace engineers studying the influence of propellant sloshing on the flight performance of space vehicles. Baffles have been used as passive slosh damping devices in the liquid storage tanks.

1.2 Background

Sloshing, the motion of the free liquid surface inside its container is one of the major concerns in design liquid storage tanks, moving tankers fuel tank space vehicles and also in ships in major cities and also in rural areas elevated water tank forms in integral part of water supply scheme and these tanks must remain functional to meet the demand in any extreme situation like earthquake, fire, etc.

Many elevated water tanks damage to their staging (support structure) in the Bhuj earthquake of January 26th 2001 and at least three of them collapsed. These water tanks are located in the area of a radius of approximately 125km from the epicenter. Tanks located in regions of the highest intensity of shaking collapsed while a few developed cracking near brace-column joint regions. Critical facilities like water tanks therefore require careful design.

1.3Linear Wave Theory

Linear wave theory is one of the first types of mathematical modelling which is used to analyze wavemotion. It is the core theory of ocean surface waves used in ocean and coastal engineering and generally used to estimate the seismic response of liquid storage tanks. It provides some understanding into wave motion at a relatively simple level. Sloshing is oftenanalyzed in a simpler form where no overturn takes place. Mathematically it is based on thegoverning equation of continuity and potential flow assumptions. Assumptions like incompressibility, irrotational flow, inviscid (viscous, drag, friction terms are neglected), no ambient velocity and small amplitudes are also allowed for a simplified analysis via linear wave theory.

Linear wave theory for a 3-D liquid container yields following equation which represents the nth mode oscillation frequency 'ω_n' in a container of length 'l' and fluid height 'h'.

$$\omega_n{}^2 = \frac{n\pi g}{l}\tanh\frac{n\pi h}{l}$$

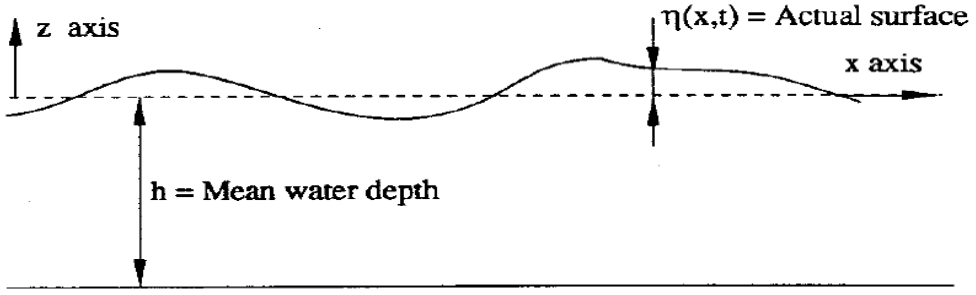

Fig 1.1 Linear Wave Motion

1.4 Fluid Structure Interaction (FSI)

Fluid-Structure Interaction refers to the coupling of unsteady fluid flow and structural deformation.
It is a two-way coupling of pressure and deflection. Its application includes airbag modelling, fueltank sloshing, heart valve modelling, helicopter crash landings, etc.
Purpose of studying FSI is that fluid mechanics may affect and be affected by the structural mechanics, and vice-versa. Hence in this case the coupling of the fluid's pressure and the motion of the structure is essential.

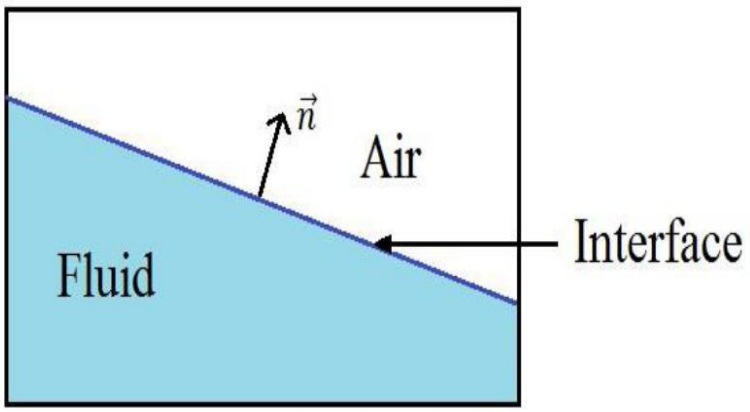

Figure 1.2: Fluid Structure Interaction

1.5 Free Surface Representation

Several techniques exist for tracking immiscible interfaces, and these can be classified under three main categories according to physical and mathematical approach:

1. Moving Grid or Lagrangian approach (Capturing)
2. Fixed grid or Eulerian Approach (Tracking)
3. Combined method of Lagrangian and Eulerian

Lagrangian approach includes moving-mesh, particle-particle scheme and boundary integral method. Eulerian approach can be divided into two main approaches: Surface tracking and Volume tracking. These include front-tracking, volume of method (VOF), Marker and Cell (MAC) method, smoothed particle hydrodynamics, level set methods, and phase field.

PHONICS, FLUENT, SRAT-CD, CFD, FLOW-3D and COMPACT. Most of them are based onthe finite volume method.

1.6 Objectives of the Present Study

The Objectives of the present study are as follows:

1) To study different aspects related to behaviour and performance of water tanks in seismic condition.

2) To study the phenomenon of sloshing in water tank and to study research efforts undertaken in the past connected to sloshing of waves.

3) Using mathematical model based on fluid mechanics background, predict these theoretically frequencies and the wave patterns.

4) Then to excite the liquid volume inside the tank at different frequencies and detect the frequencies at which standing waves are formed on the liquid surface.

5) To study the effectiveness of vertical baffle for reducing sloshing forces.

6) To check variation of baffle height relative to different liquid fill levels affecting the sloshing phenomenon, when the tank with vertical baffle at the centre of the bottom wall, is seismically excited to frequency equal to natural frequency of the liquid in the tank

CHAPTER 2

LITERATURE SURVEY

2.1 Introduction

In the current chapter, the summary of the literature surveyed during the course of this research has been presented. This survey of literature is expected to provide the background information and thus to select the objectives of the present investigation on sloshing.

2.2 Importance of sloshing

Study of sloshing was first initiated by Graham in the year 1951 when he developed an equivalent pendulum to represent the free surface oscillations of a liquid in stationary tank. Graham and Rodriguez (1952) introduced another model consisting of sloshing point mass attached with springs to the tank wall at a specified depth and a fixed rigid mass.
Initially aeronautics was the major field of interest, where the motion of fuel is studied in tanks that would adversely affect the dynamics and stability of a plane. Fuel tanks in rockets were also a major topic for study of sloshing initially. More recently, the motion of liquids, including fuels, in several naval applications and its structural & enormous effects attracted much attention.
Further fields of attention include the aerodynamic and seismic equilibrium of tall structures and its acoustical effects of fuel sloshing in vehicle fuel tanks and storage tanks.
The problem of sloshing in closed vessels has been subjected of several studies over the past few decades. The phenomenon of sloshing involves free surface movement of the fluid in the container due to sudden loads. Free surface liquid motion is very important factor in liquid storage tanks, airplanes fuel containers, space vehicles, missiles and satellites. Forces on liquid container's wall and moments will be severe when they are excited by frequencies near to resonant. Thus to avoid failures, estimation of dynamic loads is necessary.

2.3 Survey of Literature

1. Isaacson and Premasiri (2001) presented the theoretical prediction of hydrodynamic damping due to baffles in a fluid-filled rectangular tank or reservoir undergoing horizontal oscillations, and they estimated the total energy damping due to flow separation around the

baffles. In addition, they performed experimental measurements to validate the theoretical model and to investigate the effectiveness of various baffle configurations. However, these analyses are not theoretically valid for viscous and turbulent flows, so the energy dissipation and breaking waves during violent liquid sloshing cannot be described.

2. The experimental results of Akyildiz and Unal (2005) showed that the effects of the vertical baffle are most pronounced in shallow water, and that the over turning moment in particular is greatly reduced. A vertical baffle inside a tank revealed that the flow of liquid over the vertical baffle produced a shear layer, and energy was dissipated by the viscous action. These experimental results are consistent with the finding of Celebi and Akyildiz (2002) obtained through numerical investigation. Akyildiz and Unal (2006) investigated numerically an experimentally the pressure variations in both baffled and unbaffled rectangular tanks. They also confirmed that the baffles significantly reduce fluid motion and consequently pressure response.

3. Cho and Lee (2004) carried out a parametric investigation on the two-dimensional nonlinear liquid sloshing in baffled tank under horizontal forced excitation based on the fully nonlinear potential flow theory. They showed that the liquid motion and dynamic pressure variation above the baffle are more significant than those below the baffle are. In addition, they suggested that the quantities of interest in the liquid sloshing are strongly dependent on the baffle design parameters. Cho et al. (2005) adopted the numerical method proposed by Cho and Lee (2004) to research the resonance characteristics of liquid sloshing in a 2D baffled tank subjected to forced lateral excitation based on the linearized potential flow theory.

They concluded, based on a parametric examination of the effects of the height to which the liquid is filled, the number of baffles, the opening width and the baffle location, that the fundamental resonance frequency and the peak elevation height decrease uniformly with the baffle number, the baffle installation height, and the reduction of the baffle opening width and the height to which the liquid is filled. Cho and Lee (2004) and Cho et al. (2005) could not resolve the viscous sloshing and rotational motion of the liquid because sloshing flow is formulated based on the potential flow theory.

4. Younes et al. (2007) considered lower mounted and upper mounted vertical baffles of different heights and numbers to evaluate experimentally the hydrodynamic damping in partially filled rectangular tanks. They summarized their experimental results as follows. The damping ratio increases as the distance between the tip of the lower-mounted baffle plate and the liquid free surface decreases and as the distance between the plate and the center of the tank decreases. Increasing the baffle numbers increases the damping ratio. The upper mounted vertical baffles are more suitable for a chargeable tank. The twin-sided upper

mounted baffles and center-holed lower-mounted baffle arrangements yield a maximum damping ratio.

5. Liu and Lin (2009) presented a brief summary of the previous studies on baffles that were performed using the numerical approaches. In addition, they studied 3D liquid sloshing in a tank with baffles by solving the Navier–Stokes equations, and they adopted the VOF method to track the free surface motion. Their results show that, in comparison with a horizontal baffle, a vertical baffle is a more effective tool in reducing the sloshing amplitude and in deceasing the pressure exerted on the wall because of sloshing impact, even though just one baffle height of 75% of the liquid filling level was considered.

6. Panigrahy et al. (2009) showed experimentally that baffles in a tank decrease the sloshing effect considerably because sharpedged baffles create turbulence in the flow field thereby dissipating the excess kinetic energy to the walls. They used unconventional baffles in the tanks, e.g. vertical baffles with large holes and ring baffles. Their results showed that ring baffles are more effective than conventional horizontal baffles. This is because ring baffles absorb energy at all the walls and dissipate it to all the walls rather than concentrating on particular two walls normal to the direction of excitation.

7. The analysis of baffled tanks is generally very complicated and time consuming. This fact has been insisted by by Serdar Celebi & Akyildiz (2002) and Hasheminejad and Aghabeigi (2009), respectively. So it is clear that multiple baffles make the behavior of the liquid inside the tank more complicated, and accordingly makes the analysis more difficult and time consuming. In this study, a simplified method for evaluation of sloshing effects in rectangular tanks with Multiple baffle Walls (MVB) is presented. This method is based on conducting several dynamic analysis cases for tanks with various dimensions subjected to seismic excitations, and the use of neural network to create simple relationships between the dominant frequency and the amplitude of the base excitations and the maximum level of liquid in the tank.

8. Mohammed Ali Goudarzi and Saeed Reza Sabbagh Yaazdi investigated the non linear behavior of liquid sloshing inside a partially filled rectangular tank. The numerical simulations were performed for both linear and non linear conditions. In order to verify the results of the non linear numerical solution, a series of shaking table tests on rectangular tank were conducted.

Their results showed that although the wave height is limited to a practical range, the non-linear effects could increase the maximum slosh wave height up to 70%. Regardless of the base excitation input records, sloshing amplitudes oscillate predominantly at a frequency very close to the fundamental natural frequency of the contained liquid.

9. Heng Jin, Yong Liun, Hua-Jun Li studied that inner structures are often used to restrain liquid sloshing and prevent tank damage. To increase energy dissipation and reduce the forces acting on structures, a horizontal perforated plate was designed and incorporated into a rectangular liquid tank in this study. Experimental studies were conducted, and a tank with an inner submerged horizontal perforated plate was excited under different amplitudes and frequencies. The free surface elevations on the side-walls and the resonant frequencies were carefully examined. The experimental results indicate that the horizontal perforated plate can significantly restrain violent resonant sloshing in the tank under horizontal excitation.

10. Bernard Molinn, Fabien Remy studied rectangular tanks partially filled with water and fitted with vertical perforated screens proposed as Tuned Liquid Dampers to mitigate the vibratory response of land buildings, under wind or earthquake excitation. Similar devices are used as anti-rolling tanks aboard ships. Experiments are performed on a rectangular tank with one screen at mid length. The tank is subjected to forced horizontal and rolling motions, harmonic and irregular. The open-area ratio of the screen was kept constant while the motion amplitudes and frequencies were varied. Force measurements are converted into matrices of added mass/inertia and damping coefficients. A simple numerical model is proposed, based on linearised potential flow theory and quadratic discharge equation at the screen, following earlier works by the first author. Good agreement is reported between experimental and numerical hydrodynamic coefficients.

.

CHAPTER 3
MATHEMATICAL FORMULATION

3.1 Introduction

This chapter includes the details of mathematical modelling and solution methods that are generally used for study of sloshing. The mathematical equations describe the flow of liquid in case of sloshing including the motion of the free surface. It is the representation of physical event through mathematical equations. Since the physical events are difficult to model exactly, these equations provide an exact representation of reality. Computational Fluid Dynamics (CFD) techniques are used to solve the governing equation of sloshing numerically. The equations which are used to study sloshing here are: Continuity equation, Navier-stokes equation and Volume of Fluid (VOF).

3.2Continuity Equation

Continuity equation used to describe the transport of conserved quantity. It also defines the conservation of mass.
For 3-dimensional continuity equation for unsteady flow is as follow:

$$\frac{\partial \rho}{\partial t} + \frac{\partial (\rho u)}{\partial x} + \frac{\partial (\rho v)}{\partial y} + \frac{\partial (\rho w)}{\partial z} = 0$$

where, 'ρ' is the density,
'*t* ' is time,
and *u*, *v*, *w* are velocity components in *x*, *y*, *z* direction.

For incompressible and steady flow, continuity equation can be written as:

$$\frac{\partial u}{\partial x} + \frac{\partial v}{\partial y} + \frac{\partial w}{\partial z} = 0$$

3.3 Navier-Stokes Equation

Navier-Stokes equations describe the relation between velocity, pressure, temperature, viscosity and density of a moving fluid. This equation is valid for turbulent as well as laminar flow.

$$\frac{\partial(\rho u)}{\partial t}+\rho\left(u\frac{\partial u}{\partial x}+v\frac{\partial u}{\partial y}+w\frac{\partial u}{\partial z}\right)=\rho x-\frac{\partial p}{\partial x}+\frac{1}{3}\mu\frac{\partial}{\partial x}\left(\frac{\partial u}{\partial x}+\frac{\partial v}{\partial y}+\frac{\partial w}{\partial z}\right)+\mu\nabla^2 u$$

where, 'ρ is the density,
't'is time,
'*p*' is pressure,
μ is dynamic viscosity,
and *u*, *v*, *w* are velocity components in *x*, *y*, *z* direction.

3.4 Turbulence Modelling

To consider the effect of turbulence fluctuations time-average of Navier-Stokes equation should be taken, which is known as Reynolds-Averaged Navier-Stokes equation. In present study we consider *k* -ε turbulence model which assumes the relation between Reynolds stresses in the fluid and mean velocity gradients.
The turbulence viscosity can be determined by following equation:

$$\mu_t = \rho C_\mu \frac{k^2}{\varepsilon}$$

where, *k* is turbulent kinetic energy,
μ_t is turbulence viscosity,
C_μ is constant of proportionality whose default value is 0.09 in fluent,
ε is the turbulence dissipation rate.

3.5Mathematical model

Figure 3.1 shows a two-dimensional water tank of length 2*l* containing water up to a height h. We assume that the liquid flow is inviscid, irrorational, and incompressible. We now consider the question as to what type of steady state waves may exist on the liquid surface. We use the notation $\phi(x, y, t)$, $u(x, y, t)$, &$v(x, y, t)$ to represent, respectively, the velocity potential, velocity components in x and y directions.

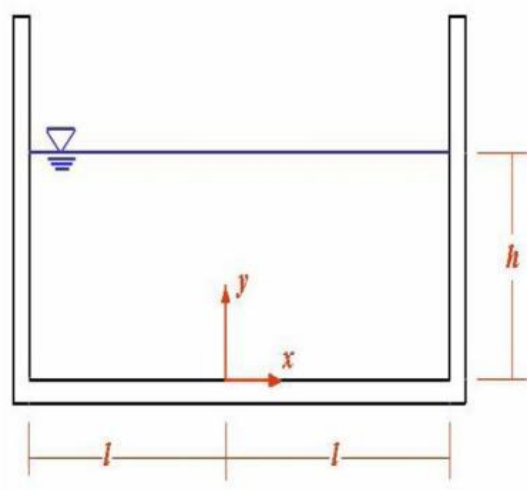

Fig 3.1 Geometry of water stored in water tank

The following equation is known to govern the velocity potential (see L G Currie, 1974, Fundamentals of mechanics of fluids, McGraw-Hill, NY, pp. 201-205) [11]

$$\frac{\partial^2\phi}{\partial x^2}+\frac{\partial^2\phi}{\partial y^2}=0$$

with the boundary conditions given by- [11]

$$\frac{\partial^2\phi}{\partial t^2}(x,h,t)+g\frac{\partial\phi}{\partial y}(x,h,t)=0$$

$$\frac{\partial\phi}{\partial y}(x,o,t)=0$$

$$\frac{\partial\phi}{\partial x}(\pm l,y,t)=0$$

The first of the above boundary conditions is obtained by applying the Bernoulli's equation on the free surface and the remaining set of boundary conditions reflects the fact that the normal fluid velocity components at the wall boundaries are zero. The symbol *g* in the above equation represents the acceleration due to gravity and the other notations are explained in figure 3.1.

We seek a steady state wave solution of the form-

$$\phi(x, y, t) = \psi(x, y)\cos\omega t$$

This leads to the field equation,

$$\frac{\partial^2\psi}{\partial x^2} + \frac{\partial^2\psi}{\partial y^2} = 0$$

with the boundary conditions-

$$-\omega^2\psi(x,h) + g\frac{\partial\psi}{\partial y}(x,h) = 0$$

$$\frac{\partial\psi}{\partial y}(x,o) = 0$$

$$\frac{\partial\psi}{\partial x}(\pm l, y) = 0$$

We seek the solution of equation in the variable separable form as $\phi(x, y) = X(x)Y(y)$. This leads to the equation,

$$\frac{d^2X}{dx^2}Y + X\frac{d^2Y}{dy^2} = 0$$

Dividing both sides by XY one gets

$$\frac{1}{X}\frac{d^2X}{dx^2} = -\frac{1}{Y}\frac{d^2Y}{dy^2}$$

This leads to,

$$\frac{d^2X}{dx^2} + \lambda^2 X = 0$$

$$\frac{d^2Y}{dy^2} - \lambda^2 Y = 0 \qquad (3.1)$$

with boundary conditions:

$$\frac{dX}{dx}(\pm l) = 0; \quad \frac{dY}{dy}(0) = 0; \quad g\frac{dY}{dy}(h) - \omega^2 y(h) = 0 \qquad (3.2)$$

From the first equation of (3.1), one gets

$$X(x) = a\cos\lambda x + b\sin\lambda x$$

Imposing the first boundary condition of equation (3.2), we will get

$$\lambda\begin{bmatrix} -\sin\lambda l & \cos\lambda l \\ \sin\lambda l & \cos\lambda l \end{bmatrix}\begin{Bmatrix} a \\ b \end{Bmatrix} = 0$$

For nontrivial solution, we will get the condition: $\lambda \sin\lambda l \cos\lambda l = 0$

This leads to two families of solutions, namely,

$$\lambda_n = \frac{n\pi}{l}; n = 1,2,3,\ldots,\infty$$

$$\lambda_m = \frac{(2m+1)\pi}{2l}; m = 0,1,2,3,\ldots,\infty$$

Considering now the second equation, we will get

$$\frac{dY}{dy}(0) = 0 \Rightarrow d\lambda = 0 \Rightarrow d = 0$$

$$g\frac{dY}{dy}(h) - \omega^2 y(h) = 0 \Rightarrow g\lambda \sinh\lambda h - \omega^2 \cosh\lambda h = 0$$

And,

$$\omega^2 = g\lambda \tanh\lambda h$$

Thus, Combining equation, we will get

$$\omega_n^2 = \frac{n\pi}{l} g \tanh\left(\frac{n\pi h}{l}\right); n = 1,2,\ldots,\infty$$

$$\omega_m^2 = \frac{(2m+1)\pi}{2l} g \tanh\left(\frac{(2m+1)\pi h}{2l}\right); m = 0,1,2,\ldots,\infty$$

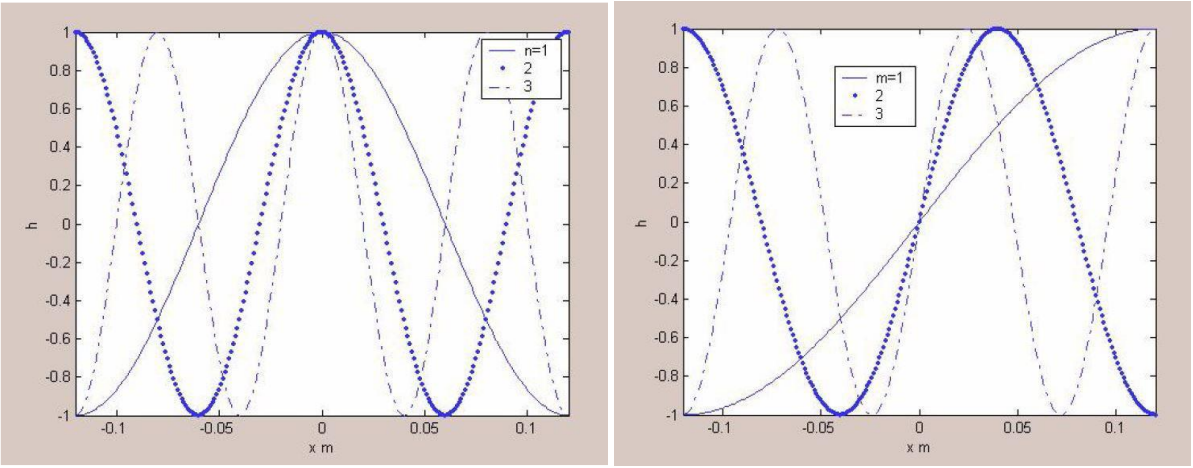

Fig 3.2 First few modes of oscillations of liquid surface obtained theoretically

Theoretical Calculations:

To get the theoretical values of natural frequencies from the equations,

$$\omega_n^2 = \frac{n\pi}{l} g \tanh\left(\frac{n\pi h}{l}\right); n = 1,2,\ldots,\infty$$

$$\omega_m^2 = \frac{(2m+1)\pi}{2l} g \tanh\left(\frac{(2m+1)\pi h}{2l}\right); m = 0,1,2,\ldots,\infty$$

And, $= \frac{\omega}{2\pi}$

And,

In our case, total length of tank = 0.3 m= 2l

i.e., l = 0.15 m

and, h = 0.25 m, g = 9.81 m/s^2

substituting these values in above equation for n = 1,2,3,……,∞ and m = 0,1,2,3,……,∞ to get two sets of solution for natural frequencies. Then we will get,

For, n = 1; ω_n 1= 205.36 rad/s thus, f_n 1= 2.28 Hz

n = 2; ω_n 2 = 410.92 rad/s f_n 2 = 3.23 Hz

n = 3; ω_n 3 = 616.38 rad/s f_n 3 = 3.95 Hz

Similarly for,

m = 0; ω_m 1= 99.66 rad/s thus, f_m 1= 1.56 Hz

m = 1; ω_m 2 = 308.19 rad/s f_m 2 = 2.79 Hz

m = 2; ω_m 3 = 513.65 rad/s f_m 3 = 3.61 Hz

m = 3; ω_m 4 = 719.11 rad/s f_m 4 = 4.27

CHAPTER 4
EXPERIMENTAL SETUP AND OBSERVATIONS

4.1 Experimental setup

The figure 4.1 shown below displays the instrumental setup of this experiment.

S.No.	Equipment	Quantity
1	Oscilloscope	1
2	Accelerometers	3
3	Shake table	1
4	Water tank model	1
5	Baffle walls	7

Table 4.1 Equipments used in conducting experiment

Fig. 4.1 Experimental setup

The physical model used for present study is shown in figure. Present model consists of a 3-dimensional liquid storage rectangular tank which is partially filled with water (ρ=999.98 kg/m^3, μ=0.00103 kg/m-s). The tank dimensions are 0.3*0.25*0.5 m^3. The rectangular walls are made up of Perspex plates housed inside a steel cage. It has a density of 1.17–1.20 g/cm^3, which is less than half that of glass. Water fill level in tank is 50% and 75% of total height of tank and the rest part is occupied with air.

In my experiment, I have used 3 different sizes of baffle walls for 50% and 75% fill water tank respectively. Fig 5.2, 5.3 and 5.4 shown below displays the different configurations of baffle walls used in our water tank model for different height of fill of water.

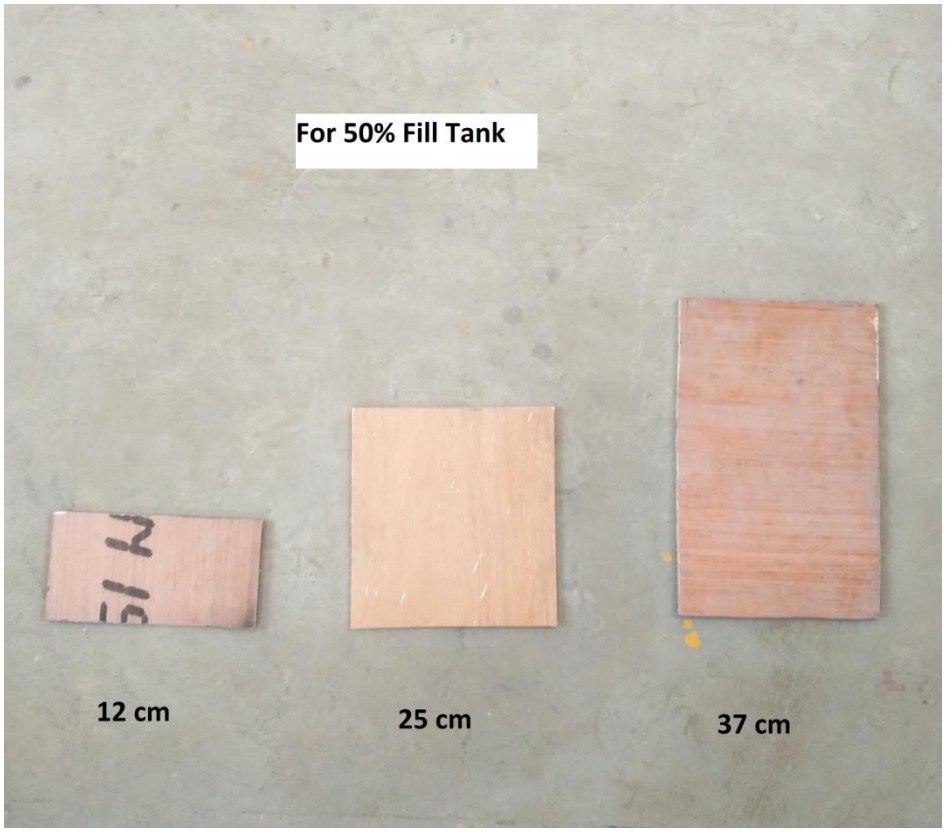

Fig 4.2 Different configurations of baffle wall for 50% fill water tank

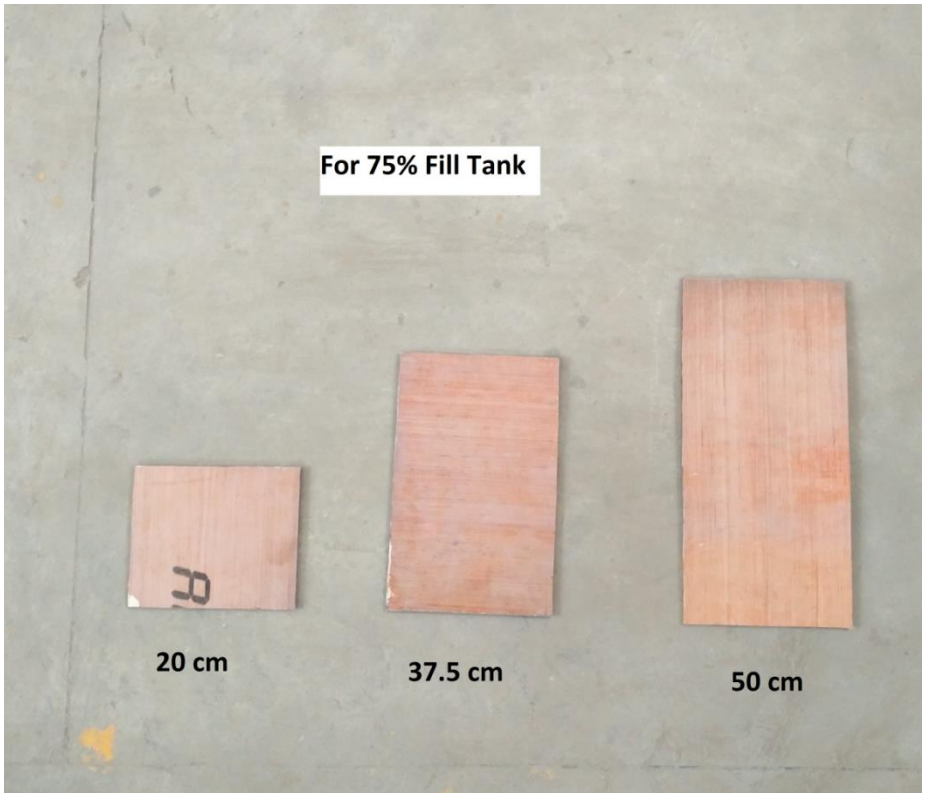

Fig 4.3 Different configurations of baffle wall for 75% fill water tank

4.2 Perforated baffle wall configurations

In my experiment, I have used 4 different perforated type baffle wall configurations which are illustrated in fig 5.4, fig 5.5, fig 5.6 and fig 5.7.

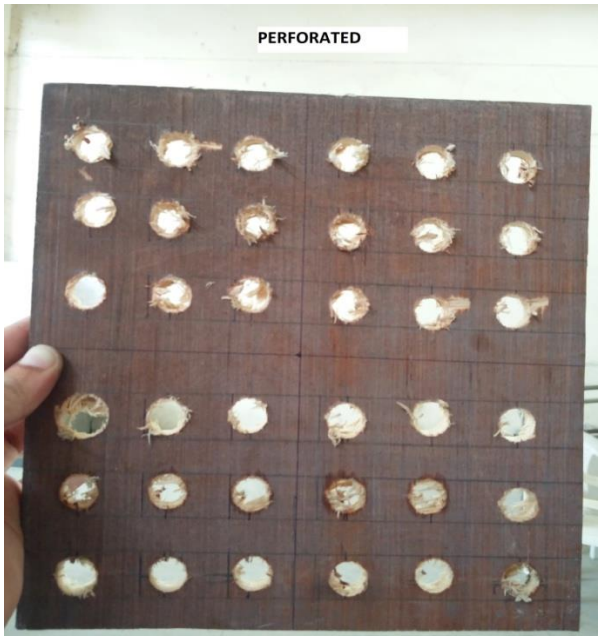

Fig 4.4 Perforated type baffle wall of size 25cm

Fig 4.5 Perforated type (I) baffle wall with top two rows of holes blocked

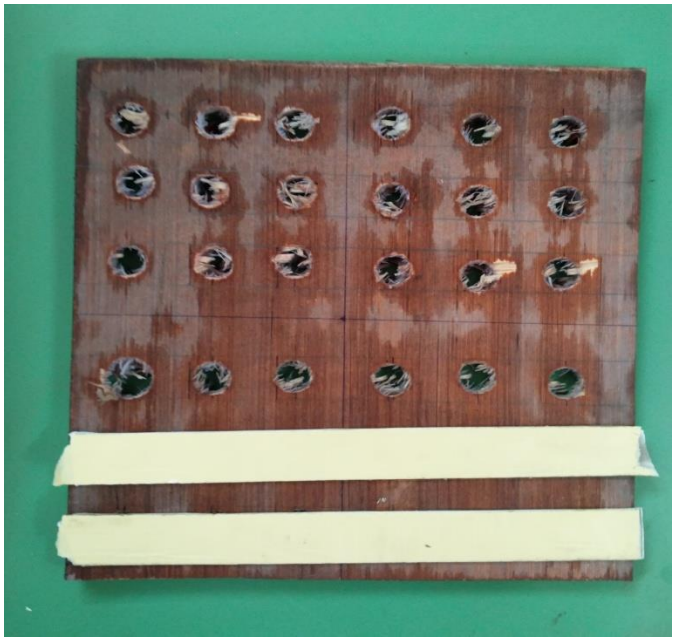

Fig 4.6 Perforated type (II) baffle wall with bottom two rows blocked

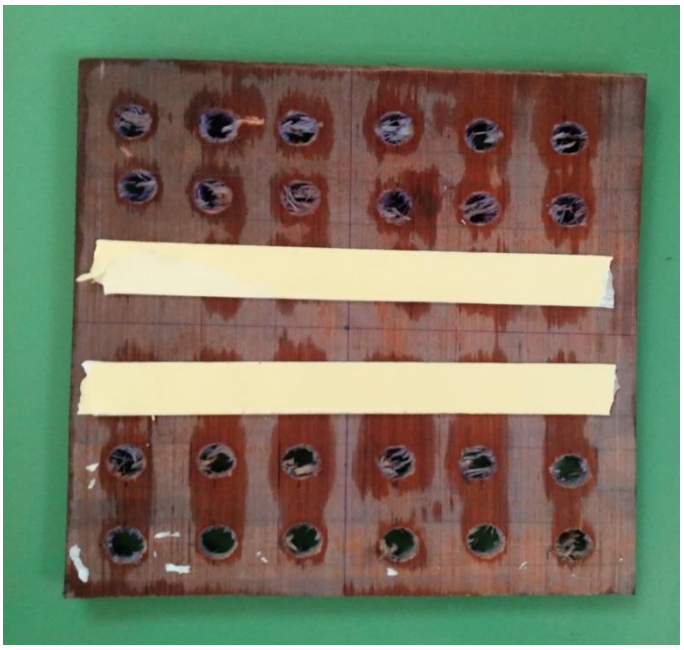

Fig 4.7 Perforated type (III) baffle wall with middle two rows blocked

4.3 Experimental Procedure

1. We mounted the water tank on the shake table as shown in figure 5.1.

2. Then we measured the dimensions of the tank and filled the water tank up to a level of 50% . A blue color dye was added to the water so as the sloshing waves could be easily observed.

3. Then the tank was excited with the help of shake table starting with low values of frequency. The water surface was observed carefully at each frequency value.

4. At every value of the frequency sufficient time was allowed to pass so that oscillations of water could reach steady state.

5. As the frequency approaches one of the natural frequencies, the water surface began to oscillate with perceptible amplitude. The frequency at which such oscillations occur were noted down. The observations were recorded as given in Tables 6.1.

6. The shape of the standing waves at the liquid surface for first few modes can be observed clearly.

7. The frequencies and shapes of the standing waves using the theoretical formulation were calculated.

8. The theoretical and experimental results are compared in chapter 6 and conclusions are drawn on their mutual agreement/disagreement.

9. The experiment was then repeated for different values of heights of water level inside the tank and readings were taken from the software and recorded in excel.

10. Then the study has been done for the following cases of seismic excitation frequency as obtained above :

(I) When the water tank is subjected to seismic excitation at first mode i.e. fn = 1.6 Hz for 50% fill water level. And at this fill level further cases are considered i.e. tank with 12 cm, 25 cm, 37 cm baffle wall and without baffle wall.

(II) When the water tank is subjected to seismic excitation at second mode i.e. fn = 2.8 Hz for 50% fill water level. And at this fill level further cases are considered i.e. tank with 12 cm, 25 cm, 37 cm baffle wall and without baffle wall.

(III) When the water tank is subjected to seismic excitation at third mode i.e. fn = 3.7 Hz for 50% fill water level. And at this fill level further cases are considered i.e. tank with 12 cm, 25 cm, 37 cm baffle wall and without baffle wall.

(IV) When the water tank is subjected to seismic excitation at fourth mode i.e. fn = 4.4 Hz for 50% fill water level. And at this fill level further cases are considered i.e. tank with 12 cm, 25 cm, 37 cm baffle wall and without baffle wall.

(V) When the water tank is subjected to seismic excitation at first mode i.e. fn = 1.6 Hz for 75% fill water level. And at this fill level further cases are considered i.e. tank with 20 cm, 37.5 cm, 50 cm baffle wall and without baffle wall.

(VI) When the water tank is subjected to seismic excitation at second mode i.e. fn = 2.8 Hz for 75% fill water level. And at this fill level further cases are considered i.e. tank with 20 cm, 37.5 cm, 50 cm baffle wall and without baffle wall.

(VII) When the water tank is subjected to seismic excitation at third mode i.e. fn = 3.7 Hz for 75% fill water level. And at this fill level further cases are considered i.e. tank with 20 cm, 37.5 cm, 50 cm baffle wall and without baffle wall.

(VIII) When the water tank is subjected to seismic excitation at fourth mode i.e. fn = 4.4 Hz for 75% fill water level. And at this fill level further cases are considered i.e. tank with 20 cm, 37.5 cm, 50 cm baffle wall and without baffle wall.

(IX) When the water tank is subjected to seismic excitation at first mode i.e. fn = 1.6 Hz for 50% fill water level. And at this fill level further cases are considered i.e. tank with 25cm baffle wall, tank with perforated baffle wall of different configurations and without baffle wall.

(X) When the water tank is subjected to seismic excitation at second mode i.e. fn = 2.8 Hz for 50% fill water level. And at this fill level further cases are considered i.e. tank with 25cm baffle wall, tank with perforated baffle wall of different configurations and without baffle wall.

(XI) When the water tank is subjected to seismic excitation at third mode i.e. fn = 3.7 Hz for 50% fill water level. And at this fill level further cases are considered i.e. tank with 25cm baffle wall, tank with perforated baffle wall of different configurations and without baffle wall.

(XII) When the water tank is subjected to seismic excitation at fourth mode i.e. fn = 4.4 Hz for 50% fill water level. And at this fill level further cases are considered i.e. tank with 25cm baffle wall, tank with perforated baffle wall of different configurations and without baffle wall.

4.4 Observations

Firstly, we need to calculate the natural frequency of the system. For calculating that we start by exciting the tank harmonically with very low frequency values and carefully observes the water surface profile. The frequencies at which the water surface began to oscillate with perceptible amplitude are noted down. All the videos showing the vibration patterns at different modes are recorded and are provided in the CD attached with this thesis.

4.4.1 The shape of the standing waves at resonance at the liquid surface for first four modes are as follows:

For observing the shape of standing waves, we oscillated the shake table at different frequencies and observed the vibration patterns very carefully.

The shape of standing waves at 50% fill tank capacity are as shown below :

Fig 4.8 Shape of standing wave at Mode 1 at frequency of 1.6 Hz

Fig 4.9 Shape of standing wave at Mode 2 at frequency of 2.8 Hz

Fig 4.10 Shape of standing wave at Mode 3 at frequency of 3.7 Hz

Fig 4.11 Shape of standing wave at Mode 4 at frequency of 4.4 Hz

The shape of the standing waves at 75% fill tank capacity are as shown below :

Fig 4.12 Shape of standing wave at Mode 1(75%) at frequency of 1.6 Hz

Fig 4.13 Shape of standing wave at Mode 2(75%) at frequency of 2.8 Hz

Fig 4.14 Shape of standing wave at Mode 3(75%) at frequency of 3.7 Hz

Fig 4.15 Shape of standing wave at Mode 3(75%) at frequency of 4.4 Hz

4.5 Readings obtained

The tank is provided with three accelerometers on wall of the tank. These accelerometers are connected to the amplifier which is connected to the computer. The software used in this study is OROS NVGate. This software records the accelerations of the surface to which the accelerometers are attached. The values of accelerations obtained are interms of factors of gravity (g). The readings are in decimal values so we have converted them into the unit mm/s^2 so as to facilitate their analysis. Input 1 is connected at the bottom, input 2 is connected in the middle and input 3 is connected at the top of the tank as shown in Fig 5.16.

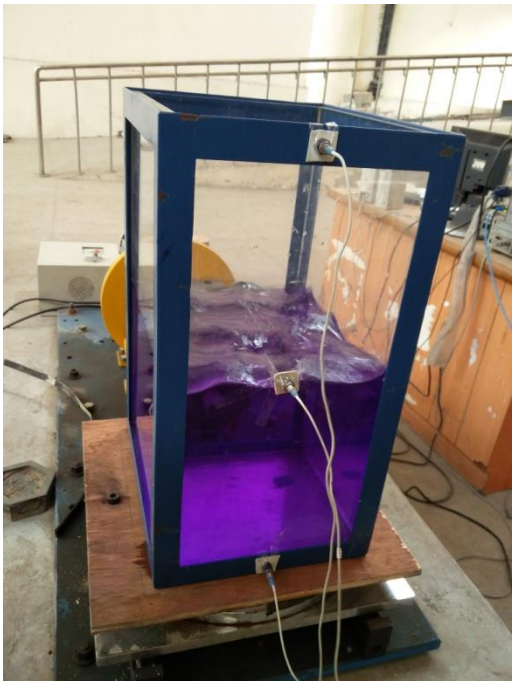

Fig 4.16 Figure showing position of three accelerometers

Then these readings are plotted on graphs with respect to time. The graphs have been plotted in excel and are given in chapter 6. The first column of the following tables consist of the time of excitation which is at 4 second interval up to 100 seconds. The second, third and fourth columns consist of values of accelerations corresponding to three accelerometers.

Table 5.2 to 5.13 provide the data obtained from the software for different cases. Each tableis given with the variation in parameters. The parameters taken into account are percentage of fill of tank, excitation frequency, presence or absence of baffle, height of baffle and type of bafflewall.

Table 4.2 Variation of acceleration with time at 50% fill without baffle at frequency 1.6 Hz

Time s	Input 1 mm/s²	Input 2 mm/s²	Input 3 mm/s²
4	205.029	589.6791	652.415
8	227.2977	457.9308	625.145
12	221.3136	550.7334	525.654
16	197.8677	599.7834	499.5252
20	219.2535	413.4915	533.9583
24	230.1426	593.2107	623.916
28	224.3547	570.6477	536.607
32	237.8925	586.638	625.2894
36	208.8549	598.9986	528.9552
40	220.8231	573.9831	501.7815
44	223.7661	577.2204	555.7365
48	223.9623	570.3534	618.1281
52	212.3865	592.6221	610.254
56	212.877	585.3627	523.1673
60	209.0511	575.5527	510.8067
64	219.5478	569.6667	523.3635
68	230.4369	593.505	564.075
72	203.8518	601.6473	581.6349
76	216.0162	527.8761	561.5244
80	232.8894	441.0576	567.4104
84	206.8929	577.0242	517.2813
88	217.0953	555.0498	586.8342
92	217.3896	424.1844	527.4837
96	207.8739	411.2352	601.8435
100	213.2694	589.7772	547.8885

Table 4.3 Variation of acceleration with time at 50% fill without baffle at frequency 2.8 Hz

Time s	Input 1 mm/s²	Input 2 mm/s²	Input 3 mm/s²
4	363.2643	886.1373	931.2633
8	453.3201	889.1784	1188.972
12	415.0611	876.5235	1084.005
16	427.9122	928.9089	1205.649
20	423.8901	884.2734	1123.245
24	464.6016	884.6658	1185.048
28	420.849	869.3622	1122.264
32	475.0983	883.5867	1261.566
36	426.0483	859.4541	1107.549
40	460.089	902.9124	1220.364
44	431.5419	846.3087	1077.138
48	438.507	878.6817	1187.991
52	468.6237	871.5204	1163.466
56	460.7757	857.9826	1075.176
60	450.5733	839.2455	1226.25
64	441.45	847.1916	1142.865
68	453.8106	869.5584	1148.751
72	406.3302	857.5902	1120.302
76	478.9242	872.3052	1213.497
80	435.1716	876.033	1187.991
84	436.7412	884.6658	1188.972
88	457.9308	847.4859	1079.1
92	407.5074	860.0427	1072.233
96	471.7629	846.9954	1229.193
100	415.8459	875.5425	1099.701

Table 4.4 Variation of acceleration with time at 50% fill without baffle at frequency 3.7 Hz

Time s	Input 1 mm/s²	Input 2 mm/s²	Input 3 mm/s²
4	558.97	1098.72	1624.536
8	532.78	1107.549	1592.163
12	556.42	1107.549	1629.441
16	561.03	1130.112	1734.408
20	556.91	1133.055	1543.113
24	570.55	1144.827	1664.757
28	588.01	1101.663	1600.011
32	527.19	1151.694	1547.037
36	553.48	1150.713	1708.902
40	557.31	1114.416	1719.693
44	560.15	1146.789	1581.372
48	557.01	1180.143	1714.788
52	530.62	1118.34	1661.814
56	558.39	1121.283	1543.113
60	565.55	1135.998	1629.441
64	580.26	1149.732	1677.51
68	573.2	1140.903	1583.334
72	556.91	1150.713	1588.239
76	578.1	1177.2	1471.5
80	567.61	1133.055	1619.631
84	574.67	1131.093	1588.239
88	550.54	1156.599	1635.327
92	557.01	1172.295	1548.999
96	556.13	1138.941	1711.845
100	571.82	1111.473	1543.113

Table 4.5 Variation of acceleration with time at 50% fill without baffle at frequency 4.4 Hz

Time s	Input 1 mm/s²	Input 2 mm/s²	Input 3 mm/s²
4	832.9671	1118.34	1690.263
8	824.8248	1121.283	1719.693
12	803.0466	1130.998	1748.142
16	804.9105	1149.732	1753.047
20	785.8791	1140.903	1724.598
24	801.0846	1137.713	1771.686
28	816.3882	1158.245	1683.396
32	815.5053	1133.055	1730.484
36	822.078	1113.093	1725.579
40	824.6286	1146.599	1722.636
44	780.7779	1152.295	1703.997
48	826.2963	1138.941	1854.09
52	782.5437	1111.473	1640.232
56	799.7112	1107.549	1773.648
60	808.9326	1107.549	1751.085
64	803.1447	1130.112	1748.142
68	829.1412	1125.055	1745.199
72	816.9768	1146.827	1781.496
76	786.2715	1101.663	1709.883
80	803.3409	1151.694	1738.332
84	809.6193	1150.713	1717.731
88	836.793	1114.416	1802.097
92	802.9485	1146.789	1717.731
96	807.0687	1180.143	1751.085
100	829.8279	1111.473	1702.035

Table 4.6 Variation of acceleration with time at 50% fill with 12cm baffle at frequency 1.6 Hz

Time s	Input 1 mm/s²	Input 2 mm/s²	Input 3 mm/s²
4	832.5747	294.4962	657.1719
8	846.9954	281.1546	575.847
12	852.0966	296.6544	627.1533
16	849.8403	316.1763	632.4507
20	846.4068	296.8506	638.7291
24	846.9954	317.1573	682.9722
28	842.679	328.3407	709.4592
32	845.1315	313.7238	670.3173
36	847.9764	301.2651	664.7256
40	843.3657	328.5369	712.0098
44	841.5018	317.0592	685.9152
48	844.2486	334.7172	709.7535
52	836.793	330.597	701.415
56	840.1284	340.3089	722.6046
60	833.9481	348.9417	681.5007
64	841.2075	294.1038	586.8342
68	836.793	309.6036	638.2386
72	834.6348	288.1197	656.4852
76	829.6317	327.9483	685.5228
80	830.6127	315.882	686.4057
84	821.9799	327.2616	724.2723
88	830.5146	324.3186	691.5069
92	828.945	314.5086	691.8012
96	827.964	332.8533	667.08
100	829.3374	310.2903	680.6178

Table 4.7 Variation of acceleration with time at 50% fill with 12cm baffle at frequency 2.8 Hz

Time s	Input 1 mm/s²	Input 2 mm/s²	Input 3 mm/s²
4	1321.407	700.9245	1143.846
8	1332.198	614.9889	960.8895
12	1317.483	621.3654	955.9845
16	1326.312	603.0207	886.4316
20	1325.331	647.8524	1081.062
24	1313.559	608.5143	1054.575
28	1332.198	630.0963	1240.965
32	1326.312	633.4317	1084.986
36	1318.464	632.5488	1057.518
40	1309.635	613.6155	1118.34
44	1319.445	626.6628	1129.131
48	1311.597	676.3995	1071.252
52	1296.882	656.1909	990.81
56	1298.844	706.9086	1012.392
60	1304.73	785.0943	965.8926
64	1317.483	679.7349	1206.63
68	1313.559	608.4162	1248.813
72	1301.787	604.4922	1097.739
76	1313.559	576.0432	1060.461
80	1308.654	559.8567	1168.371
84	1308.654	629.7039	1140.903
88	1295.901	652.9536	987.867
92	1291.977	625.6818	1007.487
96	1308.654	671.4945	936.855
100	1297.863	604.5903	1043.784

Table 4.8 Variation of acceleration with time at 50% fill with 12cm baffle at frequency 3.7 Hz

Time s	Input 1 mm/s²	Input 2 mm/s²	Input 3 mm/s²
4.000	1500.930	886.137	1226.250
8.000	1495.044	889.178	1156.599
12.000	1501.911	876.524	1211.535
16.000	1488.177	928.909	1129.131
20.000	1484.253	884.273	1146.789
24.000	1484.253	884.666	1119.321
28.000	1496.025	869.362	1135.017
32.000	1488.177	883.587	1155.618
36.000	1498.968	859.454	1144.827
40.000	1477.386	902.912	1237.041
44.000	1481.310	846.309	1233.117
48.000	1479.348	878.682	1192.896
52.000	1482.291	871.520	1229.193
56.000	1490.139	857.983	1064.385
60.000	1481.310	839.246	1139.922
64.000	1467.576	847.192	1206.630
68.000	1476.405	869.558	1110.492
72.000	1478.367	857.590	1138.941
76.000	1474.443	872.305	1179.162
80.000	1474.443	876.033	1173.276
84.000	1477.386	884.666	1127.169
88.000	1471.500	847.486	1191.915
92.000	1472.481	860.043	1148.751
96.000	1466.595	846.995	1224.288
100.000	1464.633	875.543	1205.649

Table 4.9 Variation of acceleration with time at 50% fill with 12cm baffle at frequency 4.4 Hz

Time s	Input 1 mm/s²	Input 2 mm/s²	Input 3 mm/s²
4	1632.384	988.848	1660.833
8	1666.719	1084.005	1871.748
12	1663.776	1079.1	1874.691
16	1714.788	1060.461	1722.636
20	1721.655	1061.442	1766.781
24	1765.8	1032.012	1712.826
28	1766.781	1039.86	1650.042
32	1740.294	1072.233	1831.527
36	1738.332	1078.119	1829.565
40	1750.104	1067.328	1708.902
44	1733.427	1054.575	1796.211
48	1727.541	1061.442	1869.786
52	1757.952	1028.088	1726.56
56	1736.37	1071.252	1854.09
60	1765.8	1062.423	1741.275
64	1781.496	1077.138	1811.907
68	1760.895	1067.328	1700.073
72	1762.857	1065.366	1798.173
76	1780.515	1009.449	1625.517
80	1758.933	1070.271	1780.515
84	1778.553	1069.29	1727.541
88	1757.952	1066.347	1797.192
92	1773.648	1111.473	1820.736
96	1770.705	1057.518	1710.864
100	1755.99	1070.271	1793.268

Table 4.10 Variation of acceleration with time at 50% fill with 25cm baffle at frequency 1.6 Hz

Time s	Input 1 mm/s²	Input 2 mm/s²	Input 3 mm/s²
4	869.755	299.794	540.825
8	879.270	321.964	518.360
12	891.435	258.984	528.759
16	883.783	325.398	542.395
20	881.723	299.401	544.063
24	903.795	333.050	506.981
28	904.286	297.047	515.614
32	896.144	300.971	553.480
36	918.216	309.015	517.281
40	901.539	277.525	527.189
44	903.109	280.566	554.559
48	900.166	292.338	557.993
52	916.745	359.733	539.844
56	896.536	266.342	513.848
60	888.001	281.057	575.651
64	905.757	277.133	550.635
68	892.612	290.867	587.423
72	915.175	292.829	525.326
76	904.678	282.234	516.202
80	910.859	276.642	534.155
84	898.890	269.481	570.844
88	894.574	319.217	553.775
92	900.950	308.132	512.769
96	913.703	269.677	455.773
100	894.868	297.635	564.369

Table 4.11 Variation of acceleration with time at 50% fill with 25cm baffle at frequency 2.8 Hz

Time s	Input 1 mm/s²	Input 2 mm/s²	Input 3 mm/s²
4	1084.986	588.306	1159.542
8	1180.143	550.457	871.6185
12	1171.314	565.482	1086.948
16	1116.378	484.712	1201.725
20	1048.689	586.148	782.9361
24	997.677	576.632	1147.77
28	1015.335	658.349	1095.777
32	1023.183	574.081	1177.2
36	1022.202	585.951	1181.124
40	1013.373	609.397	1114.416
44	1029.069	599.882	1145.808
48	1045.746	569.765	1112.454
52	1035.936	553.186	1177.2
56	1037.898	548.87	1137.96
60	1068.309	504.136	1144.827
64	1064.385	644.909	1105.587
68	1045.746	681.01	1155.618
72	1048.689	602.53	1158.561
76	1078.119	569.372	1075.176
80	1059.48	640.789	824.04
84	1055.556	597.233	1116.378
88	1040.841	535.724	1059.48
92	1087.929	540.041	837.0873
96	1084.005	516.3	783.2304
100	1052.613	564.762	1157.58

Table 4.12 Variation of acceleration with time at 50% fill with 25cm baffle at frequency 3.7 Hz

Time s	Input 1 mm/s²	Input 2 mm/s²	Input 3 mm/s²
4	1322.388	700.8264	1170.333
8	1327.293	687.3867	1347.894
12	1327.293	713.187	1239.984
16	1327.293	680.2254	1154.637
20	1315.521	687.7791	1215.459
24	1320.426	682.776	1332.198
28	1321.407	684.2475	1255.68
32	1311.597	690.9183	1134.036
36	1327.293	705.1428	1312.578
40	1303.749	722.3103	1149.732
44	1318.464	728.1963	1160.523
48	1320.426	721.4274	1226.25
52	1318.464	731.9241	1212.516
56	1302.768	669.2382	1144.827
60	1309.635	678.0672	1189.953
64	1305.711	723.978	1225.269
68	1320.426	672.1812	1260.585
72	1310.616	695.4309	1197.801
76	1310.616	717.3072	1203.687
80	1312.578	698.7663	1220.364
84	1308.654	676.7919	1176.219
88	1313.559	722.997	1096.758
92	1323.369	689.5449	1242.927
96	1319.445	718.2882	1135.017
100	1306.692	720.8388	1173.276

Table 4.13 Variation of acceleration with time at 50% fill with 25cm baffle at frequency 4.4 Hz

Time s	Input 1 mm/s²	Input 2 mm/s²	Input 3 mm/s²
4	1526.436	1011.411	1879.596
8	1529.379	989.829	1721.655
12	1536.246	1038.879	1717.731
16	1528.398	1036.917	1933.551
20	1538.208	1017.297	1807.983
24	1526.436	1020.24	1740.294
28	1545.075	1033.974	1878.615
32	1519.569	989.829	1656.909
36	1524.474	1046.727	1779.534
40	1531.341	1032.993	1792.287
44	1522.512	989.829	1520.55
48	1541.151	1071.252	2027.727
52	1542.132	1022.202	1740.294
56	1541.151	1011.411	1773.648
60	1518.588	997.677	1659.852
64	1540.17	1039.86	1842.318
68	1523.493	1011.411	1672.605
72	1525.455	1019.259	1784.439
76	1525.455	989.829	1586.277
80	1531.341	1031.031	1811.907
84	1529.379	1023.183	1803.078
88	1529.379	1053.594	1859.976
92	1526.436	1022.202	1869.786
96	1520.55	986.886	1656.909
100	1517.607	994.734	1795.23

Table 4.14 Variation of acceleration with time at 50% fill with 37cm baffle at frequency 1.6 Hz

Time	Input 1	Input 2	Input 3
s	mm/s²	mm/s²	mm/s²
4	1220.364	218.4687	676.89
8	1213.497	216.3105	666.1971
12	1225.269	221.2155	545.6322
16	1212.516	221.2155	781.9551
20	1233.117	229.0635	690.0354
24	1222.326	210.7188	741.9303
28	1221.345	223.4718	647.8524
32	1241.946	233.3799	664.2351
36	1216.44	204.048	697.1967
40	1230.174	226.8072	587.2266
44	1216.44	233.0856	648.441
48	1214.478	227.9844	593.7012
52	1193.877	234.2628	737.5158
56	1226.25	228.0825	603.7074
60	1235.079	258.003	605.0808
64	1217.421	242.4051	540.8253
68	1197.801	260.6517	638.4348
72	1211.535	224.2566	693.567
76	1224.288	218.8611	582.8121
80	1201.725	219.5478	612.9288
84	1210.554	245.25	639.2196
88	1206.63	238.5792	627.3495
92	1189.953	211.3074	628.4286
96	1219.383	192.0798	631.5678
100	1201.725	256.3353	601.5492

Table 4.15 Variation of acceleration with time at 50% fill with 37cm baffle at frequency 2.8 Hz

Time	Input 1	Input 2	Input 3
s	mm/s²	mm/s²	mm/s²
4	1518.588	589.6791	1409.697
8	1526.436	457.9308	1090.872
12	1537.227	550.7334	1220.364
16	1548.999	581.5485	1032.993
20	1543.113	413.4915	1181.124
24	1529.379	593.2107	1056.537
28	1527.417	570.6477	1153.656
32	1541.151	586.638	1204.668
36	1526.436	575.6584	1180.143
40	1527.417	573.9831	1088.91
44	1517.607	577.2204	1109.511
48	1498.968	570.3534	1238.022
52	1525.455	592.6221	1220.364
56	1524.474	585.3627	1444.032
60	1487.196	575.5527	1485.234
64	1545.075	569.6667	1189.953
68	1540.17	593.505	1096.758
72	1542.132	601.6473	1126.188
76	1544.094	527.8761	1052.613
80	1537.227	441.0576	973.0539
84	1529.379	577.0242	1115.397
88	1512.702	555.0498	1209.573
92	1522.512	424.1844	1201.725
96	1510.74	411.2352	1233.117
100	1518.588	589.7772	1066.347

Table 4.16 Variation of acceleration with time at 50% fill with 37cm baffle at frequency 3.7 Hz

Time	Input 1	Input 2	Input 3
s	mm/s²	mm/s²	mm/s²
4	1779.534	558.9738	1511.721
8	1773.648	532.7811	1466.595
12	1768.743	556.4232	1517.607
16	1772.667	561.0339	1552.923
20	1779.534	556.9137	1504.854
24	1772.667	570.5496	1529.379
28	1771.686	588.0114	1429.317
32	1763.838	527.1894	1439.127
36	1760.895	553.4802	1432.26
40	1758.933	557.3061	1467.576
44	1766.781	560.151	1407.735
48	1772.667	557.0118	1461.69
52	1762.857	530.6229	1442.07
56	1771.686	558.3852	1444.032
60	1761.876	565.5465	1394.001
64	1759.914	580.2615	1441.089
68	1754.028	573.1983	1460.709
72	1768.743	556.9137	1424.412
76	1753.047	578.1033	1447.956
80	1759.914	567.6066	1440.108
84	1755.009	574.6698	1462.671
88	1756.971	550.5372	1385.172
92	1759.914	557.0118	1394.001
96	1752.066	556.1289	1405.773
100	1755.009	571.8249	1457.766

Table 4.17 Variation of acceleration with time at 50% fill with 37cm baffle at frequency 4.4 Hz

Time	Input 1	Input 2	Input 3
s	mm/s²	mm/s²	mm/s²
4	2048.328	987.867	1838.394
8	2051.271	1014.354	1817.793
12	2051.271	1036.917	1879.596
16	2053.233	1036.917	1885.482
20	2057.157	1038.879	1971.81
24	2051.271	1050.651	1916.874
28	2038.518	987.867	1827.603
32	2048.328	1022.202	1932.57
36	2044.404	996.696	1924.722
40	2046.366	1013.373	1905.102
44	2044.404	1028.088	1824.66
48	2060.1	1044.765	1988.487
52	2049.309	991.791	1938.456
56	2051.271	1038.879	1893.33
60	2045.385	1030.05	2056.176
64	2031.651	1043.784	1973.772
68	2034.594	1013.373	1949.247
72	2020.86	1049.67	1914.912
76	2021.841	1026.126	2065.005
80	2007.126	1037.898	1913.931
84	2018.898	1014.354	1927.665
88	2013.012	1052.613	2013.993
92	2032.632	1023.183	2020.86
96	2029.689	1048.689	1939.437
100	2032.632	991.791	1861.938

Table 4.18 Variation of acceleration with time at 75% fill without baffle at frequency 1.6 Hz

Time	Input 1	Input 2	Input 3
s	mm/s²	mm/s²	mm/s²
4	523.2654	469.1142	466.956
8	535.4298	483.2406	525.1293
12	523.3635	497.4651	476.5698
16	547.1037	504.9207	492.2658
20	528.6609	536.9013	458.3232
24	534.4488	489.9114	487.7532
28	539.6481	513.5535	456.4593
32	532.2906	445.9626	428.0103
36	542.2968	477.2565	437.526
40	534.9393	466.4655	448.1208
44	526.8951	493.0506	419.7699
48	529.0533	486.0855	510.4143
52	530.8191	469.899	429.678
56	533.8602	485.7912	537.0975
60	530.2305	507.4713	437.6241
64	533.5659	506.6865	464.8959
68	531.6039	484.9083	471.9591
72	535.7241	466.3674	461.1681
76	533.0754	475.1964	505.1169
80	528.1704	481.9653	463.7187
84	528.3666	497.7594	437.9184
88	527.0913	449.6904	450.279
92	535.2336	462.6396	468.918
96	536.4108	450.8676	434.8773
100	586.5399	475.0983	454.9878

Table 4.19 Variation of acceleration with time at 75% fill without baffle at frequency 2.8 Hz

Time	Input 1	Input 2	Input 3
s	mm/s²	mm/s²	mm/s²
4	436.4469	654.7194	875.5425
8	453.4182	656.5833	941.0733
12	520.911	657.0738	1013.373
16	545.5341	637.65	1024.164
20	519.93	633.9222	1045.746
24	496.5822	655.2099	956.6712
28	506.2941	663.3522	1037.898
32	407.2131	663.8427	858.5712
36	487.0665	643.3398	925.3773
40	410.9409	645.0075	894.9663
44	485.3988	646.5771	986.886
48	477.4527	647.9505	961.8705
52	492.2658	660.8016	937.6398
56	466.5636	644.6151	955.5921
60	521.1072	639.612	1034.955
64	462.9339	669.2382	958.5351
68	455.6745	649.7163	959.5161
72	419.7699	635.0994	886.9221
76	461.4624	654.4251	927.8298
80	482.9463	653.9346	954.4149
84	502.6644	655.4061	989.829
88	443.6082	644.9094	867.6945
92	429.5799	655.1118	872.3052
96	439.5861	624.7008	877.7988
100	464.994	661.0959	930.0861

Table 4.20 Variation of acceleration with time at 75% fill without baffle at frequency 3.7 Hz

Time	Input 1	Input 2	Input 3
s	mm/s²	mm/s²	mm/s²
4	518.0661	803.439	1098.72
8	506.8827	768.7116	1071.252
12	539.3538	758.0187	1113.435
16	510.9048	765.0819	1051.632
20	496.8765	772.8318	1007.487
24	521.4996	786.5658	1090.872
28	555.246	758.5092	1146.789
32	518.3604	775.8729	1101.663
36	484.614	748.6011	1030.05
40	501.0948	802.8504	1047.708
44	526.4046	768.0249	1079.1
48	499.6233	773.7147	1038.879
52	531.2115	775.3824	1102.644
56	489.8133	757.2339	1023.183
60	499.2309	777.7368	1019.259
64	500.31	761.9427	1085.967
68	519.2433	758.2149	1073.214
72	530.6229	794.5119	1051.632
76	507.177	760.7655	1068.309
80	502.0758	753.5061	1054.575
84	541.512	761.3541	1093.815
88	536.4108	768.8097	1074.195
92	539.3538	753.1137	1098.72
96	519.3414	786.2715	1016.316
100	509.5314	760.3731	1064.385

Table 4.21 Variation of acceleration with time at 75% fill without baffle at frequency 4.4 Hz

Time	Input 1	Input 2	Input 3
s	mm/s²	mm/s²	mm/s²
4	1128.15	1166.409	2074.815
8	1085.967	1231.155	1956.114
12	1084.986	1207.611	1988.487
16	1101.663	1197.801	2043.423
20	1114.416	1222.326	2042.442
24	1115.397	1194.858	2012.031
28	1094.796	1195.839	2015.955
32	1134.036	1169.352	2147.409
36	1096.758	1172.295	2077.758
40	1099.701	1198.782	2046.366
44	1111.473	1172.295	2070.891
48	1103.625	1219.383	2013.012
52	1128.15	1197.801	2109.15
56	1110.492	1206.63	2142.504
60	1093.815	1189.953	2048.328
64	1095.777	1187.01	1979.658
68	1102.644	1208.592	2012.031
72	1115.397	1187.01	2079.72
76	1114.416	1187.991	2030.67
80	1124.226	1202.706	2085.606
84	1115.397	1196.82	2074.815
88	1083.024	1183.086	1996.335
92	1118.34	1186.029	2112.093
96	1111.473	1197.801	2062.062
100	1124.226	1185.048	2080.701

Table 4.22 Variation of acceleration with time at 75% fill with 20cm baffle at frequency 1.6 Hz

Time	Input 1	Input 2	Input 3
s	mm/s²	mm/s²	mm/s²
4	944.0163	193.4532	393.381
8	955.1016	260.4555	475.1964
12	956.3769	240.1488	436.9374
16	950.7852	254.7657	483.5349
20	931.3614	244.269	460.7757
24	929.8899	252.7056	493.6392
28	931.5576	262.1232	494.2278
32	927.5355	241.7184	439.3899
36	933.7158	242.8956	463.8168
40	923.5134	252.7056	477.8451
44	930.2823	245.4462	458.9118
48	936.2664	240.0507	440.2728
52	936.4626	246.7215	457.2441
56	933.0291	246.6234	485.3988
60	928.7127	223.4718	434.8773
64	927.4374	217.0953	426.4407
68	924.0039	226.1205	434.9754
72	932.8329	261.5346	475.3926
76	921.5514	256.6296	485.3988
80	913.8996	221.9022	440.469
84	930.2823	226.4148	454.5954
88	925.4754	240.1488	449.1999
92	916.5483	225.2376	424.1844
96	939.6018	208.6587	419.6718
100	927.8298	258.2973	478.2375

Table 4.23 Variation of acceleration with time at 75% fill with 20cm baffle at frequency 2.8 Hz

Time	Input 1	Input 2	Input 3
s	mm/s²	mm/s²	mm/s²
4	1179.162	434.0925	787.4487
8	1183.086	480.0033	858.2769
12	1193.877	468.8199	865.242
16	1197.801	495.6012	914.8806
20	1180.143	444.9816	791.8632
24	1181.124	451.4562	818.5464
28	1192.896	492.1677	904.5801
32	1175.238	478.0413	839.9322
36	1197.801	490.1076	903.8934
40	1174.257	459.7947	782.1513
44	1196.82	509.7276	933.0291
48	1184.067	445.1778	804.8124
52	1187.01	465.3864	840.717
56	1176.219	434.6811	767.0439
60	1171.314	406.3302	724.4685
64	1185.048	478.3356	856.9035
68	1181.124	478.2375	847.9764
72	1184.067	458.0289	819.135
76	1189.953	469.6047	850.7232
80	1217.421	504.1359	901.2447
84	1212.516	477.3546	864.261
88	1203.687	447.336	811.1889
92	1208.592	466.5636	835.6158
96	1186.029	417.0231	729.5697
100	1188.972	415.1592	713.2851

Table 4.24 Variation of acceleration with time at 75% fill with 20cm baffle at frequency 3.7 Hz

Time	Input 1	Input 2	Input 3
s	mm/s²	mm/s²	mm/s²
4	979.959	671.8869	1022.202
8	982.683	655.7004	995.715
12	984.045	675.7128	1048.689
16	986.088	694.9404	1083.024
20	977.916	670.1211	1007.487
24	979.278	676.7919	1023.183
28	975.192	679.7349	1056.537
32	974.511	676.5957	1049.67
36	967.701	658.4472	1019.259
40	979.278	672.2793	1032.012
44	975.873	665.9028	1018.278
48	970.425	665.7066	1025.145
52	965.658	671.2002	1028.088
56	980.64	689.643	1107.549
60	970.425	661.4883	1041.822
64	973.149	685.8171	1084.986
68	968.382	677.3805	1075.176
72	973.83	679.1463	1029.069
76	969.744	660.213	1022.202
80	969.744	670.4154	1036.917
84	965.658	666.1971	1017.297
88	960.21	643.9284	949.1175
92	960.21	662.175	1023.183
96	970.425	663.8427	1010.43
100	960.891	698.2758	1080.081

Table 4.25 Variation of acceleration with time at 75% fill with 20cm baffle at frequency 4.4 Hz

Time	Input 1	Input 2	Input 3
s	mm/s^2	mm/s^2	mm/s^2
4	1729.503	995.715	1822.698
8	1756.971	1013.373	1998.297
12	1758.933	1028.088	2023.803
16	1765.8	1014.354	1919.817
20	1735.389	1027.107	1943.361
24	1741.275	1004.544	1814.85
28	1748.142	1030.05	1922.76
32	1736.37	999.639	1794.249
36	1701.054	1027.107	1799.154
40	1736.37	1039.86	1960.038
44	1698.111	995.715	1747.161
48	1708.902	1020.24	1807.002
52	1708.902	1033.974	1874.691
56	1688.301	1013.373	1746.18
60	1706.94	1032.012	1877.634
64	1711.845	1021.221	1892.349
68	1679.472	1028.088	1758.933
72	1704.978	1028.088	1895.292
76	1716.75	1032.993	1934.532
80	1681.434	1034.955	1821.717
84	1699.092	1032.993	1893.33
88	1696.149	1017.297	1809.945
92	1684.377	1013.373	1752.066
96	1671.624	1018.278	1726.56
100	1708.902	1029.069	1774.629

Table 4.26 Variation of acceleration with time at 75% fill with 37.5cm baffle at frequency 1.6 Hz

Time	Input 1	Input 2	Input 3
s	mm/s²	mm/s²	mm/s²
4	946.8612	247.5063	411.4314
8	948.5289	229.4559	395.2449
12	946.0764	233.7723	406.7226
16	952.1586	240.8355	361.2042
20	936.855	214.7409	412.1181
24	950.0004	202.086	392.0076
28	950.0004	225.4338	406.3302
32	941.9562	231.7122	340.7994
36	938.5227	203.4594	378.5679
40	947.3517	231.516	338.8374
44	934.9911	215.2314	424.2825
48	930.969	225.8262	406.2321
52	939.9942	221.4117	381.1185
56	939.1113	231.2217	361.7928
60	927.6336	241.7184	385.2387
64	940.8771	231.516	365.0301
68	912.2319	227.1996	436.2507
72	923.2191	214.9371	397.7955
76	942.4467	223.3737	389.0646
80	937.9341	215.4276	374.0553
84	934.3044	212.9751	376.0173
88	922.7286	204.1461	374.0553
92	923.9058	223.2756	386.1216
96	906.7383	227.1015	433.0134
100	915.7635	219.2535	428.3046

Table 4.27 Variation of acceleration with time at 75% fill with 37.5cm baffle at frequency 2.8 Hz

Time	Input 1	Input 2	Input 3
s	mm/s²	mm/s²	mm/s²
4	1259.604	522.2844	1006.506
8	1227.231	429.1875	798.2397
12	1221.345	389.457	707.301
16	1229.193	381.9033	686.7
20	1224.288	347.8626	601.2549
24	1226.25	396.1278	726.4305
28	1208.592	391.7133	711.5193
32	1207.611	352.8657	656.0928
36	1247.832	558.5814	1087.929
40	1235.079	540.531	1035.936
44	1219.383	450.9657	855.6282
48	1203.687	370.4256	665.2161
52	1216.44	457.3422	870.6375
56	1204.668	374.3496	660.0168
60	1191.915	350.0208	596.448
64	1199.763	353.5524	651.0897
68	1198.782	339.8184	567.6066
72	1206.63	395.5392	728.0982
76	1200.744	347.3721	618.2262
80	1220.364	482.4558	934.9911
84	1228.212	561.4263	1061.442
88	1231.155	559.9548	1085.967
92	1197.801	346.8816	620.7768
96	1222.326	563.6826	1066.347
100	1187.01	346.8816	591.1506

Table 4.28 Variation of acceleration with time at 75% fill with 37.5cm baffle at frequency 3.7 Hz

Time	Input 1	Input 2	Input 3
s	mm/s²	mm/s²	mm/s²
4	1449.918	676.5957	1121.283
8	1448.937	690.9183	1131.093
12	1445.994	696.8043	1124.226
16	1448.937	701.0226	1165.428
20	1425.393	648.441	987.867
24	1422.45	646.2828	1024.164
28	1439.127	673.7508	1076.157
32	1433.241	692.586	1098.72
36	1435.203	686.3076	1090.872
40	1425.393	652.8555	1016.316
44	1429.317	678.1653	1098.72
48	1445.013	701.6112	1139.922
52	1434.222	680.0292	1107.549
56	1440.108	713.9718	1139.922
60	1437.165	706.4181	1134.036
64	1418.526	673.8489	1040.841
68	1431.279	695.529	1106.568
72	1424.412	676.7919	1075.176
76	1427.355	671.4945	1080.081
80	1431.279	699.2568	1138.941
84	1445.994	698.7663	1125.207
88	1434.222	661.2921	1054.575
92	1448.937	683.3646	1076.157
96	1450.899	670.9059	1088.91
100	1455.804	704.7504	1129.131

Table 4.29 Variation of acceleration with time at 75% fill with 37.5cm baffle at frequency 4.4 Hz

Time	Input 1	Input 2	Input 3
s	mm/s²	mm/s²	mm/s²
4	1827.603	1032.993	2023.803
8	1834.47	1016.316	2136.618
12	1834.47	1023.183	2121.903
16	1845.261	1033.974	2127.789
20	1827.603	1039.86	1996.335
24	1845.261	1029.069	2302.407
28	1826.622	1025.145	2159.181
32	1829.565	1056.537	2062.062
36	1828.584	1050.651	2132.694
40	1838.394	1033.974	2212.155
44	1823.679	1035.936	2004.183
48	1821.717	1034.955	2128.77
52	1826.622	1046.727	2027.727
56	1826.622	1043.784	2059.119
60	1831.527	1029.069	2167.029
64	1838.394	1026.126	2083.644
68	1831.527	1033.974	2095.416
72	1831.527	1032.993	1949.247
76	1813.869	1032.993	1892.349
80	1839.375	1046.727	2046.366
84	1849.185	1037.898	2182.725
88	1824.66	1028.088	2172.915
92	1823.679	1047.708	1931.589
96	1832.508	1035.936	2080.701
100	1827.603	1048.689	2091.492

Table 4.30 Variation of acceleration with time at 75% fill with 50cm baffle at frequency 1.6 Hz

Time	Input 1	Input 2	Input 3
s	mm/s²	mm/s²	mm/s²
4	1065.366	192.8646	560.0529
8	1103.625	179.7192	457.9308
12	1085.967	190.314	531.6039
16	1092.834	172.7541	540.7272
20	1082.043	192.6684	546.1227
24	1111.473	181.1907	469.9971
28	1088.91	190.2159	498.6423
32	1085.967	165.2985	544.7493
36	1090.872	179.4249	527.778
40	1072.233	170.4978	603.4131
44	1084.005	189.2349	588.1095
48	1087.929	197.2791	544.455
52	1084.986	181.6812	480.8862
56	1085.967	174.618	555.0498
60	1082.043	185.8995	585.2646
64	1066.347	177.0705	629.2134
68	1059.48	209.7378	556.8156
72	1095.777	192.1779	434.9754
76	1086.948	179.8173	433.7982
80	1086.948	187.0767	474.7059
84	1077.138	188.1558	575.9451
88	1080.081	184.7223	580.9482
92	1088.91	189.8235	538.2747
96	1069.29	200.124	645.3018
100	1073.214	209.1492	561.132

Table 4.31 Variation of acceleration with time at 75% fill with 50cm baffle at frequency 2.8 Hz

Time	Input 1	Input 2	Input 3
s	mm/s²	mm/s²	mm/s²
4	1391.058	496.9746	833.85
8	1380.267	489.3228	769.9869
12	1384.191	460.7757	706.9086
16	1386.153	484.9083	795.4929
20	1384.191	485.595	726.4305
24	1382.229	447.7284	768.8097
28	1381.248	443.0196	741.3417
32	1386.153	462.5415	742.617
36	1385.172	504.6264	923.121
40	1373.4	514.7307	873.09
44	1376.343	508.5504	948.4308
48	1369.476	500.31	914.4882
52	1384.191	457.2441	811.0908
56	1383.21	438.507	669.7287
60	1362.609	486.7722	829.2393
64	1365.552	464.013	795.8853
68	1374.381	482.4558	764.6895
72	1380.267	467.3484	756.1548
76	1381.248	457.5384	696.3138
80	1365.552	443.6082	691.605
84	1373.4	492.6582	893.7891
88	1371.438	485.7912	810.6984
92	1367.514	479.1204	845.5239
96	1365.552	455.184	660.6054
100	1378.305	513.1611	889.6689

Table 4.32 Variation of acceleration with time at 75% fill with 50cm baffle at frequency 3.7 Hz

Time	Input 1	Input 2	Input 3
s	mm/s²	mm/s²	mm/s²
4	1670.643	654.7194	1283.148
8	1653.966	656.5833	1200.744
12	1655.928	657.0738	1131.093
16	1659.852	637.65	1160.523
20	1652.004	633.9222	1186.029
24	1645.137	655.2099	1232.136
28	1659.852	663.3522	1159.542
32	1648.08	663.8427	1194.858
36	1644.156	643.3398	1128.15
40	1639.251	645.0075	1272.357
44	1645.137	646.5771	1147.77
48	1638.27	647.9505	1226.25
52	1640.232	660.8016	1193.877
56	1647.099	644.6151	1143.846
60	1634.346	639.612	1239.984
64	1637.289	669.2382	1217.421
68	1641.213	649.7163	1178.181
72	1630.422	635.0994	1265.49
76	1640.232	654.4251	1141.884
80	1645.137	653.9346	1174.257
84	1652.004	655.4061	1115.397
88	1628.46	644.9094	1187.01
92	1638.27	655.1118	1163.466
96	1645.137	624.7008	1178.181
100	1652.004	661.0959	1160.523

Table 4.33 Variation of acceleration with time at 75% fill with 50cm baffle at frequency 4.4 Hz

Time	Input 1	Input 2	Input 3
s	mm/s²	mm/s²	mm/s²
4	2065.005	965.6964	2284.749
8	2097.378	968.0508	2311.236
12	2076.777	962.0667	2198.421
16	2074.815	955.2978	2126.808
20	2064.024	939.3075	2312.217
24	2053.233	985.905	2131.713
28	2051.271	961.1838	2190.573
32	2053.233	968.7375	2054.214
36	2049.309	971.6805	2058.138
40	2043.423	994.734	2150.352
44	2043.423	962.2629	2103.264
48	2039.499	970.6014	2308.293
52	2038.518	965.1078	2233.737
56	2047.347	978.6456	2276.901
60	2039.499	980.2152	2277.882
64	2032.632	966.1869	2165.067
68	2029.689	964.9116	2241.585
72	2035.575	946.4688	2248.452
76	2034.594	935.5797	2176.839
80	2045.385	961.1838	2198.421
84	2037.537	961.4781	2302.407
88	2037.537	979.4304	2215.098
92	2026.746	951.8643	2177.82
96	2028.708	980.2152	2181.744
100	2025.765	1001.601	2229.813

Table 4.34 Variation of acceleration with time at 50% fill with perforated baffle wall at frequency 1.6 Hz

Time	Input 1	Input 2	Input 3
s	mm/s²	mm/s²	mm/s²
4	239.4621	283.1166	626.7609
8	224.3547	258.003	588.4038
12	216.7029	255.9429	572.5116
16	230.535	276.8382	634.1184
20	225.1395	259.8669	573.885
24	199.6335	242.9937	525.4236
28	209.8359	251.0379	548.8695
32	210.8169	264.4776	589.581
36	222.0003	272.1294	599.0967
40	210.7188	250.3512	560.9358
44	208.3644	245.9367	561.6225
48	229.0635	290.8665	640.8873
52	216.2124	257.2182	560.9358
56	203.2632	258.6897	555.246
60	225.0414	287.3349	647.2638
64	204.1461	256.3353	567.4104
68	219.2535	280.1736	617.3433
72	220.0383	294.3981	626.2704
76	194.5323	229.9464	511.5915
80	218.3706	273.3066	599.6853
84	216.0162	264.0852	590.0715
88	211.0131	266.6358	618.1281
92	232.3989	271.0503	633.6279
96	215.3295	272.8161	598.0176
100	194.9247	253.9809	542.2968

Table 4.35 Variation of acceleration with time at 50% fill with perforated baffle wall at frequency 2.8 Hz

Time	Input 1	Input 2	Input 3
s	mm/s²	mm/s²	mm/s²
4	476.766	533.9583	1107.549
8	427.6179	456.8517	918.5103
12	349.4322	459.5985	856.5111
16	469.2123	559.2681	1138.941
20	345.1158	439.8804	856.6092
24	339.7203	440.8614	847.0935
28	471.4686	574.3755	1187.01
32	350.0208	453.6144	847.7802
36	341.1918	437.0355	859.5522
40	519.3414	569.8629	1249.794
44	346.6854	401.6214	770.1831
48	439.3899	516.987	985.905
52	379.1565	436.8393	844.9353
56	433.4058	494.8164	1032.012
60	316.2744	408.5865	763.0218
64	333.7362	402.6024	814.7205
68	334.9134	407.5074	726.1362
72	326.0844	423.5958	816.4863
76	343.0557	416.7288	800.5941
80	374.4477	453.4182	864.5553
84	435.1716	485.4969	1006.506
88	346.8816	416.7288	788.4297
92	351.5904	405.3492	783.2304
96	457.6365	488.6361	1033.974
100	368.6598	458.2251	882.8019

Table 4.36 Variation of acceleration with time at 50% fill with perforated baffle wall at frequency 3.7 Hz

Time	Input 1	Input 2	Input 3
s	mm/s^2	mm/s^2	mm/s^2
4	560.9358	701.2188	1146.789
8	544.455	718.7787	1187.991
12	545.3379	704.5542	1161.504
16	540.4329	705.1428	1166.409
20	533.4678	698.1777	1136.979
24	535.1355	686.6019	1119.321
28	525.4236	688.9563	1097.739
32	552.2049	717.6996	1177.2
36	538.6671	718.7787	1184.067
40	555.8346	724.7628	1211.535
44	534.4488	710.6364	1153.656
48	541.0215	712.3041	1199.763
52	550.0467	720.2502	1208.592
56	549.4581	727.902	1199.763
60	522.1863	680.0292	1071.252
64	521.4015	673.4565	1048.689
68	516.3003	694.8423	1109.511
72	537.4899	704.2599	1138.941
76	539.4519	717.111	1164.447
80	567.6066	728.0982	1239.984
84	526.2084	698.8644	1111.473
88	520.5186	675.7128	1078.119
92	556.3251	703.8675	1151.694
96	546.0246	722.8008	1213.497
100	540.7272	695.4309	1140.903

Table 4.37 Variation of acceleration with time at 50% fill with perforated baffle wall at frequency 4.4 Hz

Time	Input 1	Input 2	Input 3
s	mm/s²	mm/s²	mm/s²
4	822.078	1041.822	1651.023
8	820.2141	1025.145	1612.764
12	823.8438	1029.069	1613.745
16	815.8977	1016.316	1581.372
20	841.8942	1032.012	1657.89
24	825.4134	1030.05	1612.764
28	865.6344	1055.556	1647.099
32	831.0051	1031.031	1600.011
36	839.4417	1025.145	1564.695
40	859.6503	1060.461	1737.351
44	826.2963	1029.069	1621.593
48	830.4165	1025.145	1600.011
52	835.6158	1037.898	1668.681
56	832.5747	1026.126	1600.992
60	838.9512	1025.145	1557.828
64	830.907	1032.012	1597.068
68	848.0745	1032.012	1602.954
72	848.4669	1042.803	1677.51
76	841.3056	1024.164	1611.783
80	803.7333	1005.525	1535.265
84	830.907	1022.202	1600.992
88	888.2955	1071.252	1755.009
92	854.0586	1069.29	1808.964
96	837.0873	1039.86	1601.973
100	836.2044	1024.164	1548.018

CHAPTER 5

RESULTS AND DISCUSSION

5.1 Comparison between Theoretical and Experimental Natural Frequencies of the Water Tank System

Table 5.1 Comparison between Theoretical and Experimental Natural Frequency

Mode	Theoretical Frequency	Experimental Frequency
1	1.56	1.6
2	2.78	2.8
3	3.61	3.7
4	4.27	4.4

From Table 5.1, a good agreement between theoretical and experimental natural frequencies is reported. At this frequency, resonance conditions appear and water surface is found to oscillate with perceptible amplitude.

5.2 Comparison between All inputs for 50% fill and 75% fill without baffle wall

5.2.1 Comparison between all inputs for 50% fill for all 4 modal frequencies

5.2.1.1 For frequency 1.6 Hz

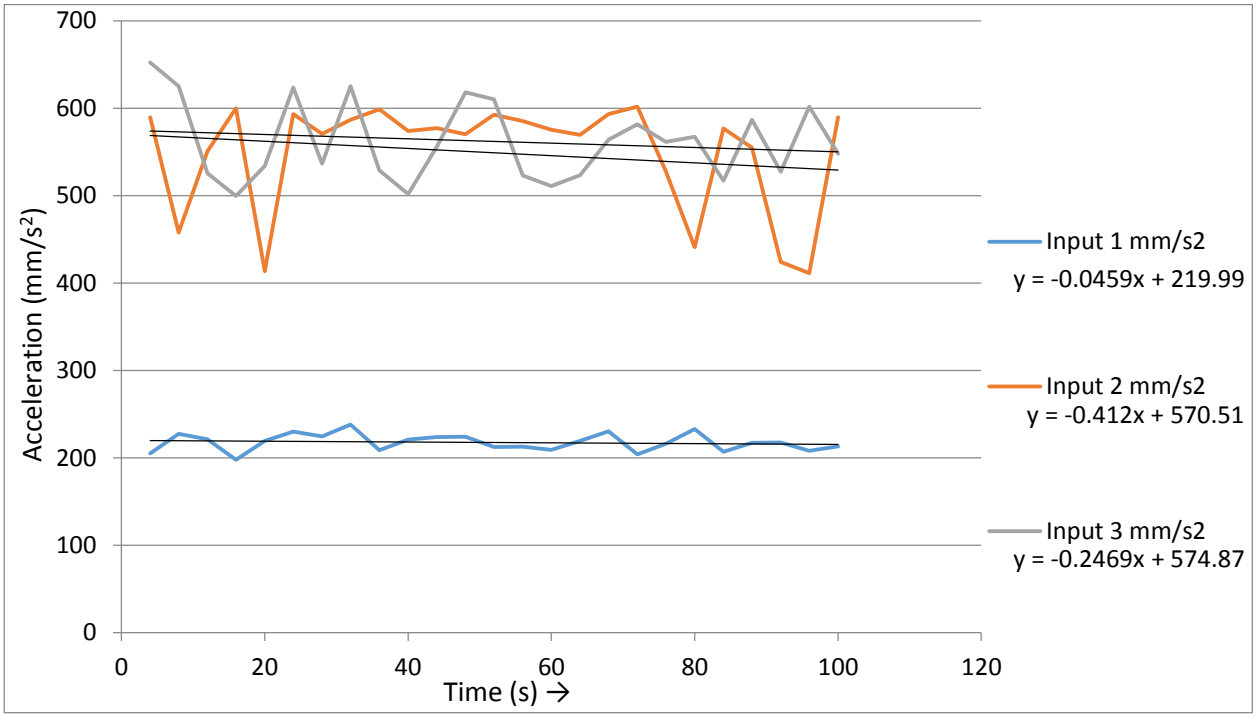

Fig 5.1 Comparison between all inputs for 50% fill at frequency 1.6 Hz

5.2.1.2 For frequency 2.8 Hz

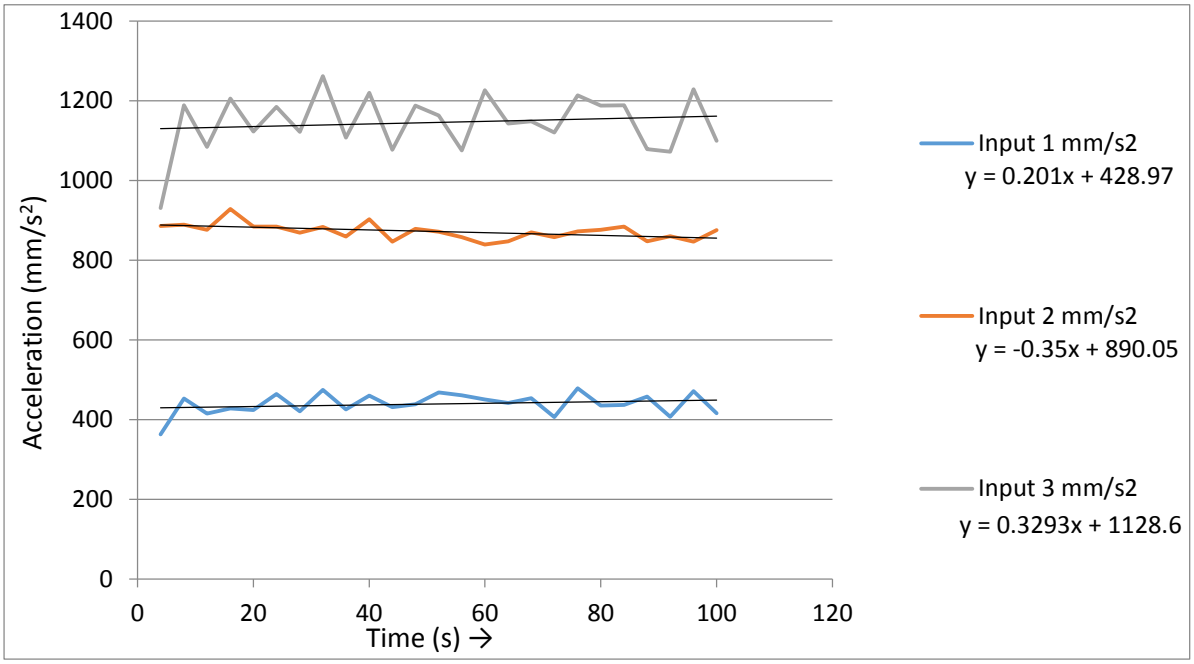

Fig 5.2 Comparison between all inputs for 50% fill at frequency 2.8 Hz

5.2.1.3 For frequency 3.7 Hz

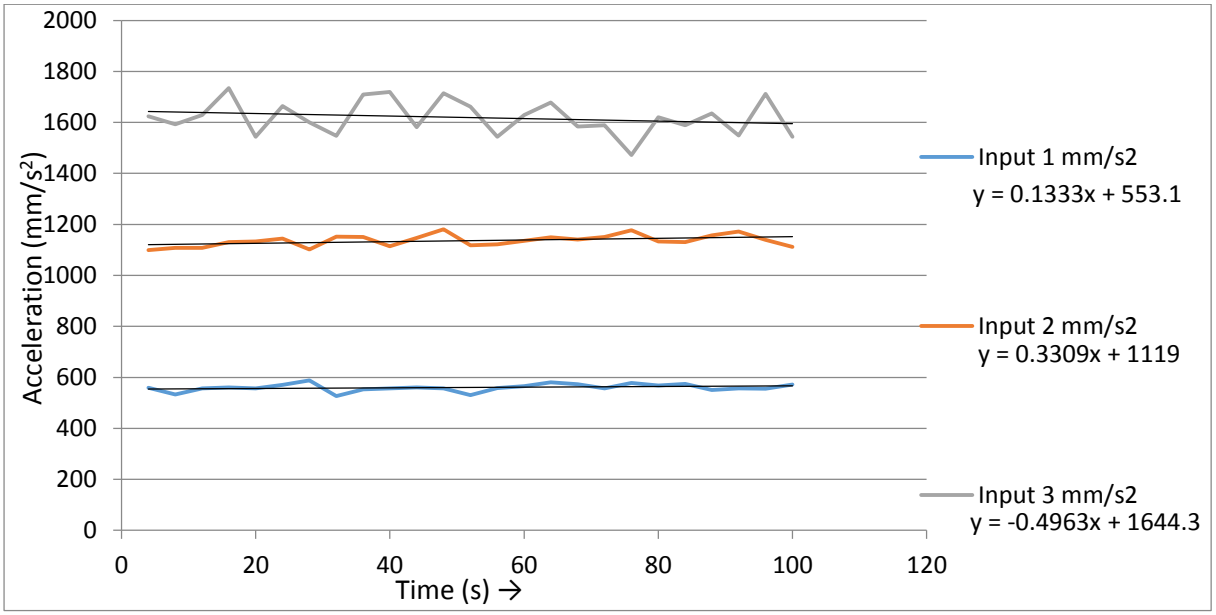

Fig 5.3Comparison between all inputs for 50% fill at frequency 3.7 Hz

5.2.1.4 For frequency 4.4 Hz

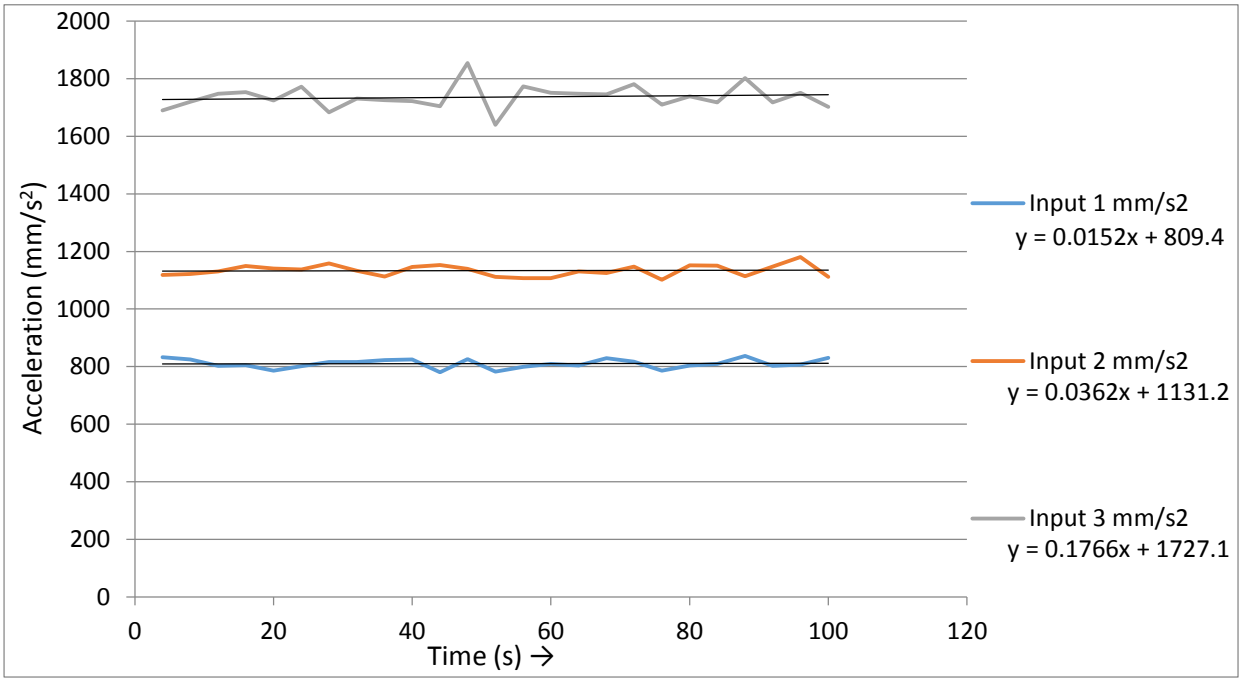

Fig 5.4 Comparison between all inputs for 50% fill at frequency 4.4 Hz

From the above 4 graphs, it is clear that acceleration value increases in magnitude with the increase in height of position of accelerometer from bottom, that is, Input 3 value is greater than Input 2 value which, in turn, is greater than Input 1 value for all the 4 values of modal frequencies.

5.2.2 Comparison between all inputs for 75% fill for all 4 modal frequencies

5.2.2.1 For frequency 1.6 Hz

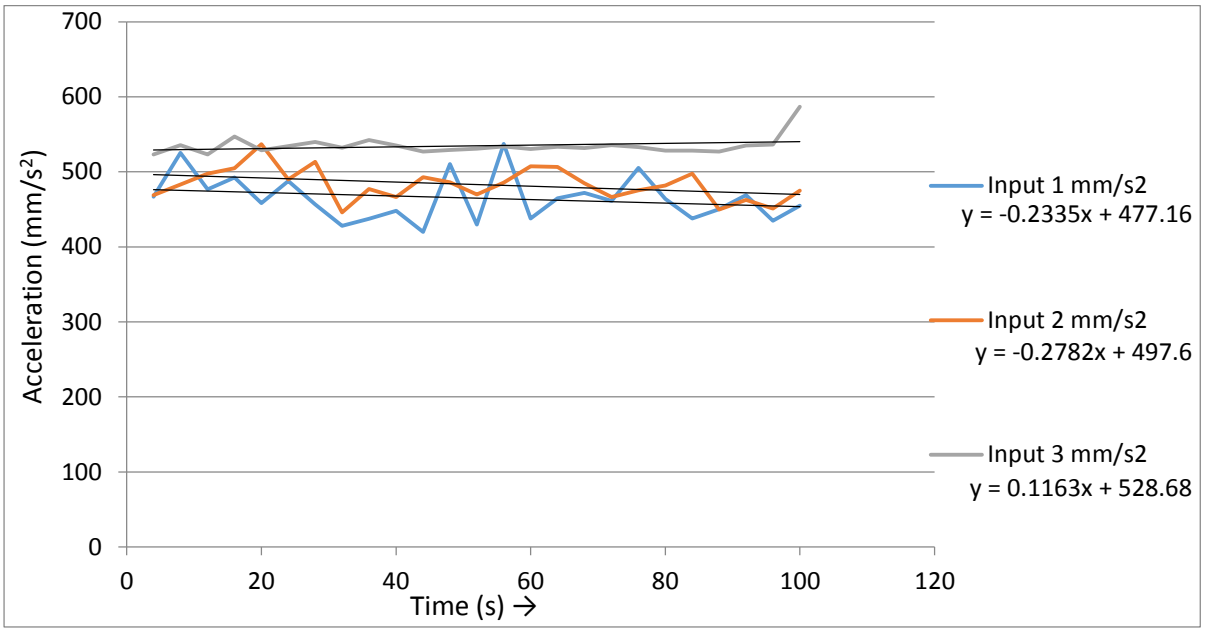

Fig 5.5 Comparison between all inputs for 75% fill at frequency 1.6 Hz

5.2.2.2 For frequency 2.8 Hz

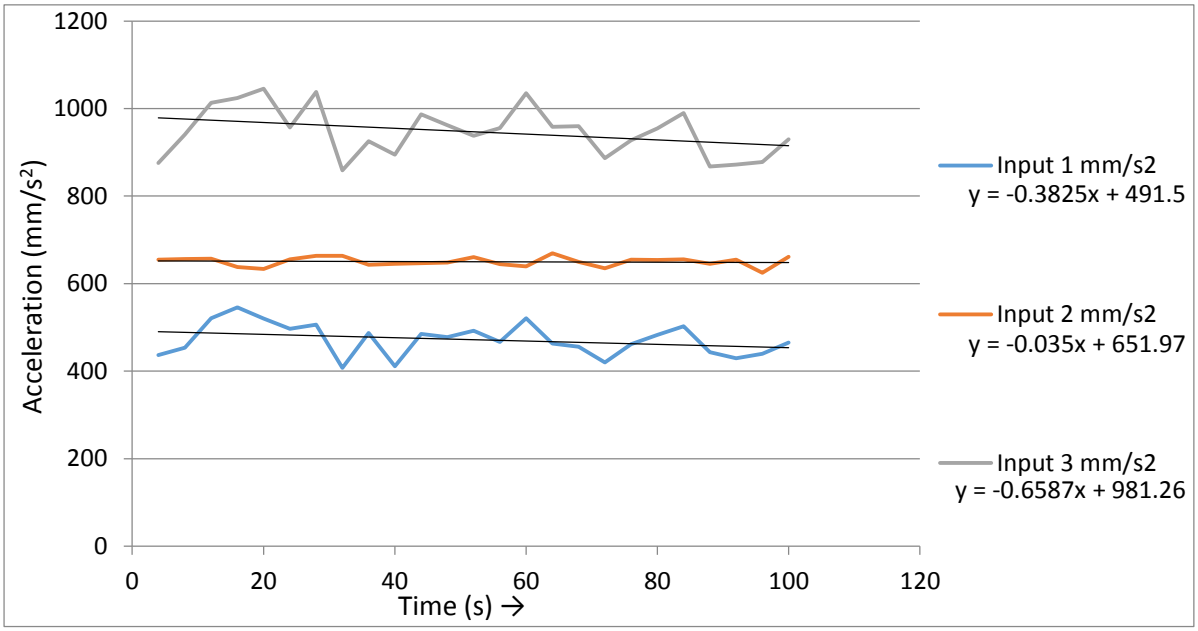

Fig 5.6 Comparison between all inputs for 75% fill at frequency 2.8 Hz

5.2.2.3 For frequency 3.7 Hz

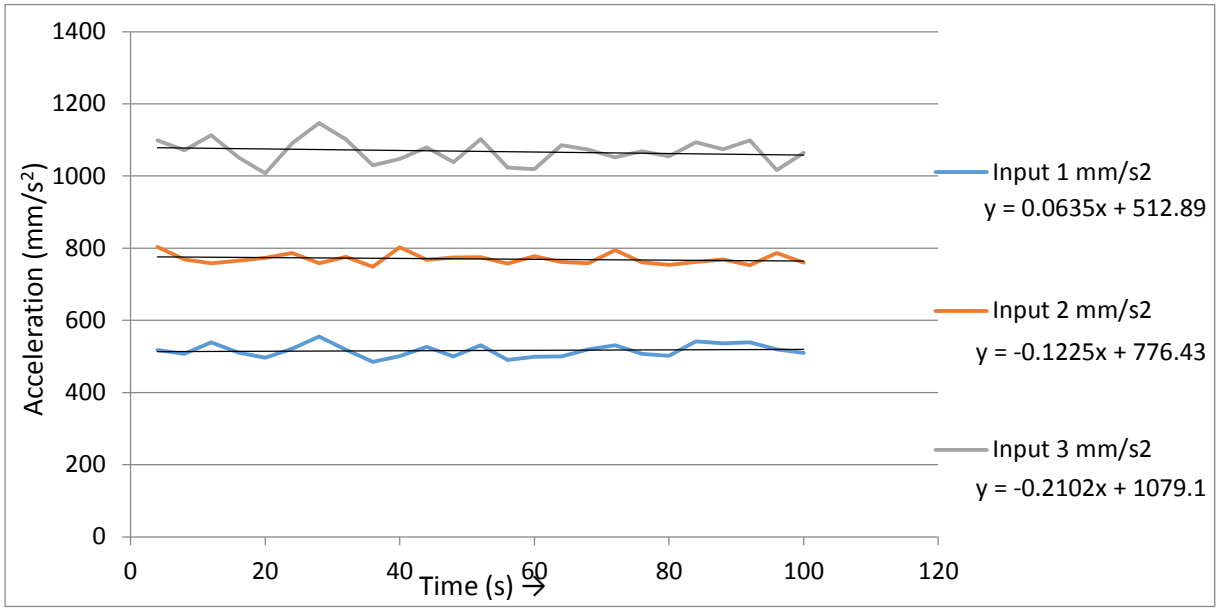

Fig 5.7 Comparison between all inputs for 75% fill at frequency 3.7 Hz

5.2.2.4 For frequency 4.4 Hz

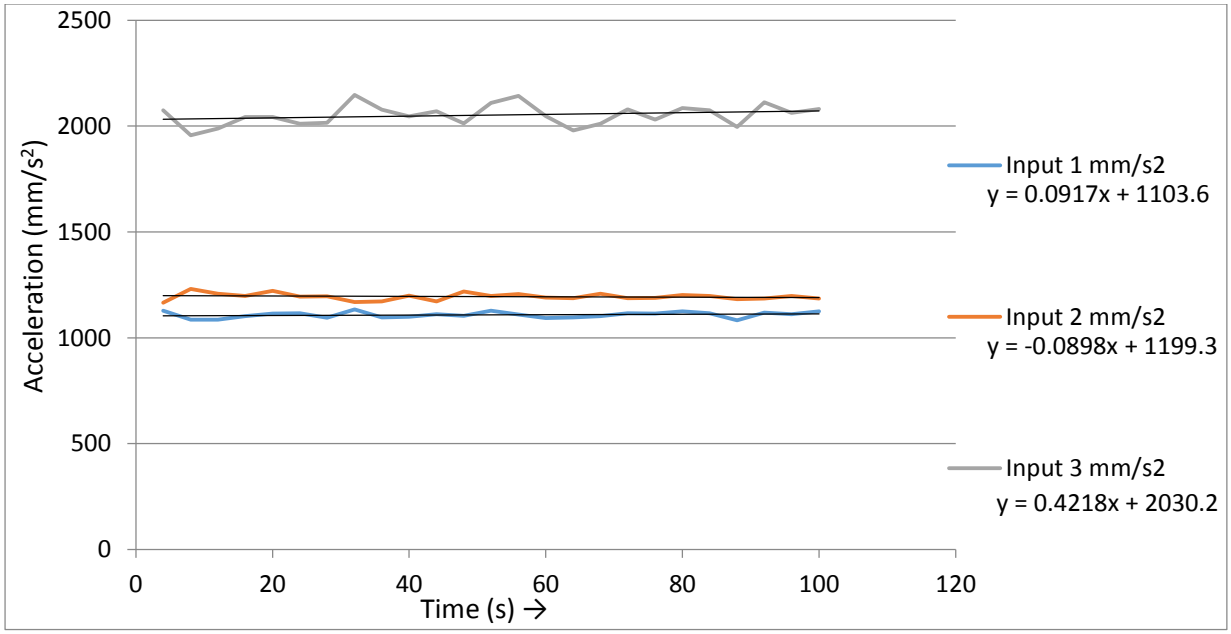

Fig 5.8 Comparison between all inputs for 75% fill at frequency 4.4 Hz

From the above 4 graphs, it is clear that acceleration value increases in magnitude with the increase in height of position of accelerometer from bottom, that is, Input 3 value is greater than Input 2 value which, in turn, is greater than Input 1 value for all the 4 values of modal frequencies.

5.3 Comparison between acceleration for each frequency

This section compares the Input 2 (acceleration values in mm/s^2) for all the 4 modal frequencies value for both 50% and 75% fill water tank capacity with and without baffle walls.

5.3.1 For 50% fill water tank capacity

5.3.1.1 For 50% fill and frequency of 1.6 Hz

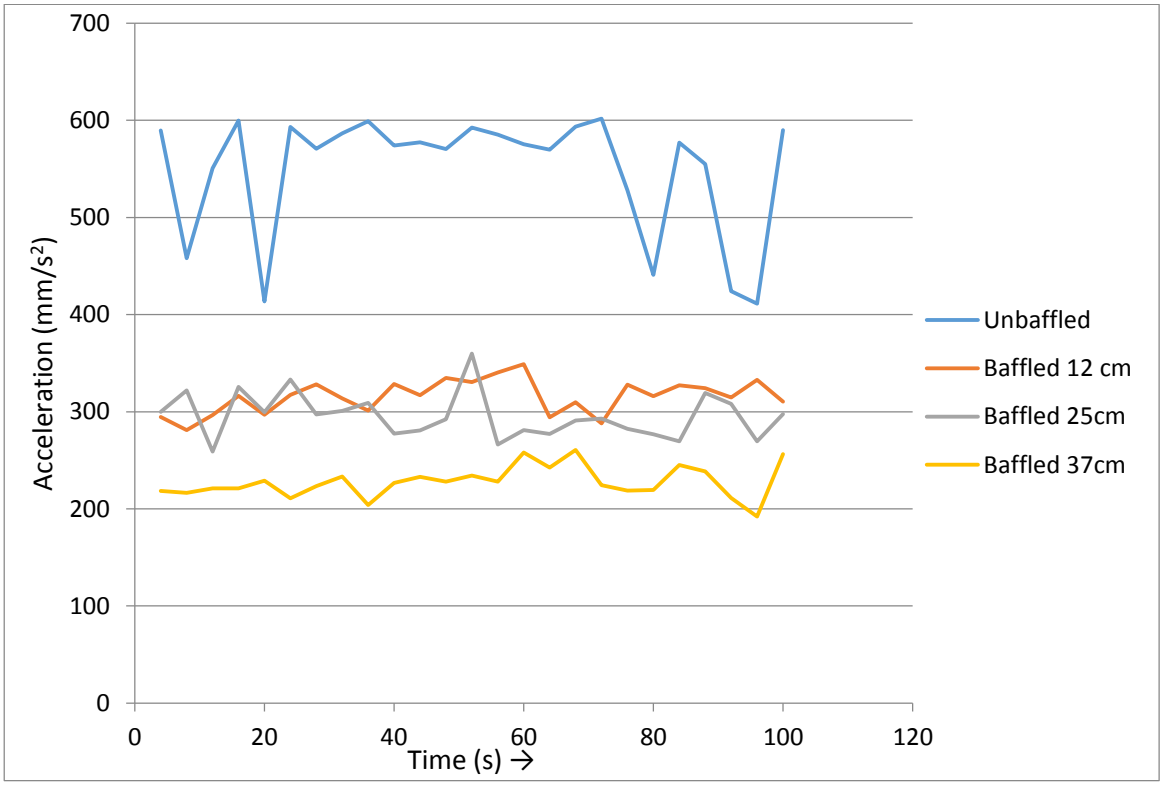

Fig 5.9 Comparison between acceleration for 50% fill for frequency 1.6 Hz

5.3.1.2 For 50% fill and frequency of 2.8 Hz

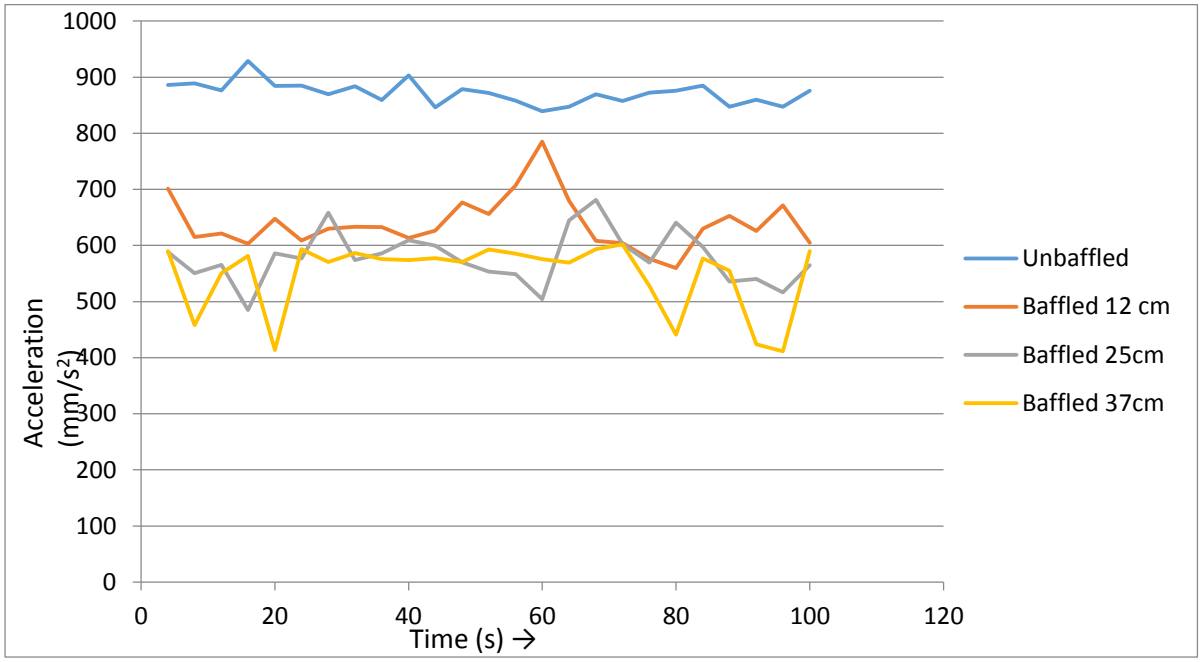

Fig 5.10 Comparison between acceleration at 50% fill for frequency 2.8 Hz

5.3.1.3 For 50% fill and frequency of 3.7 Hz

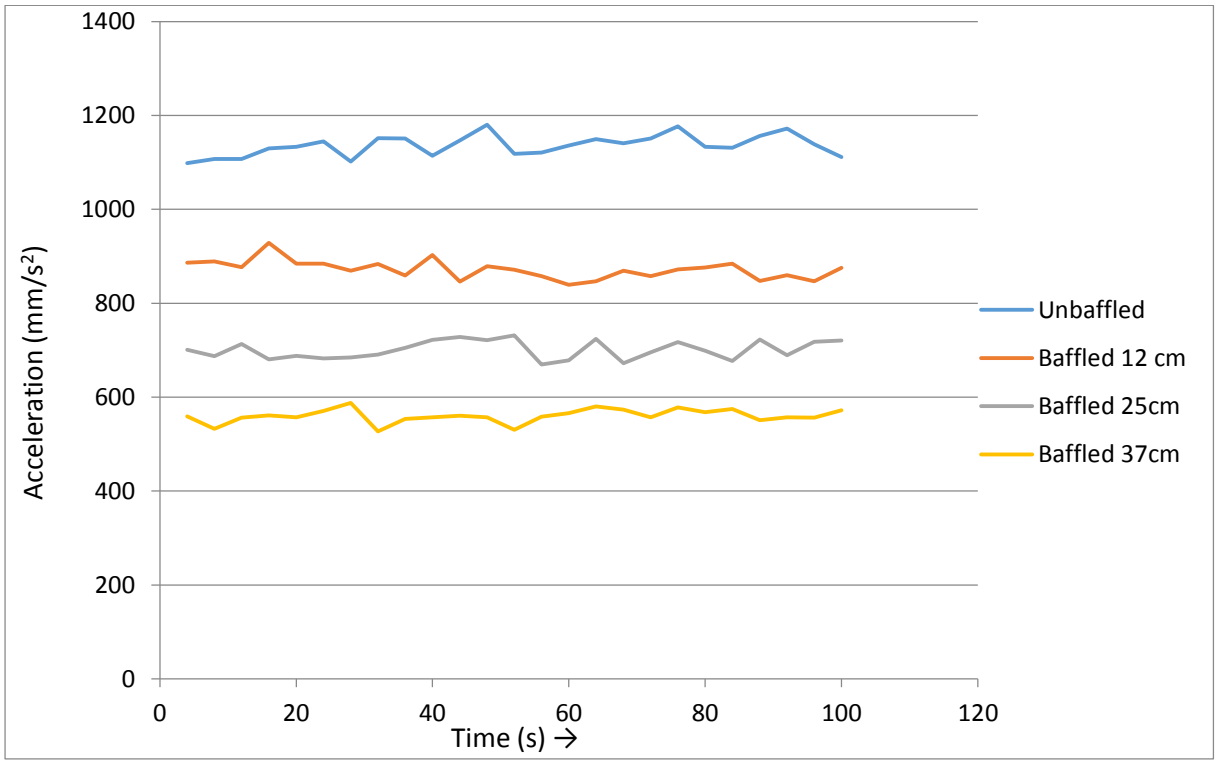

Fig 5.11 Comparison between acceleration at 50% fill for frequency 3.7 Hz

5.3.1.4 For 50% fill and frequency of 4.4 Hz

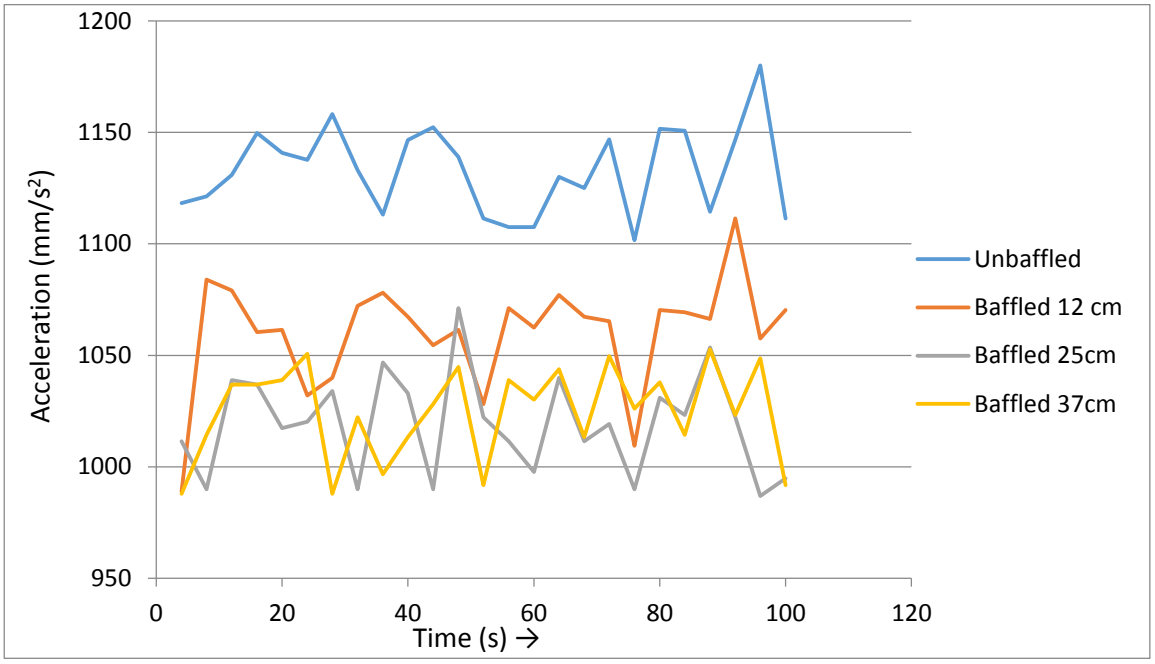

Fig 5.12 Comparison between acceleration for 50% fill for frequency 4.4 Hz

5.3.2 For 75% fill water tank capacity

5.3.2.1 For 75% fill and frequency of 1.6 Hz

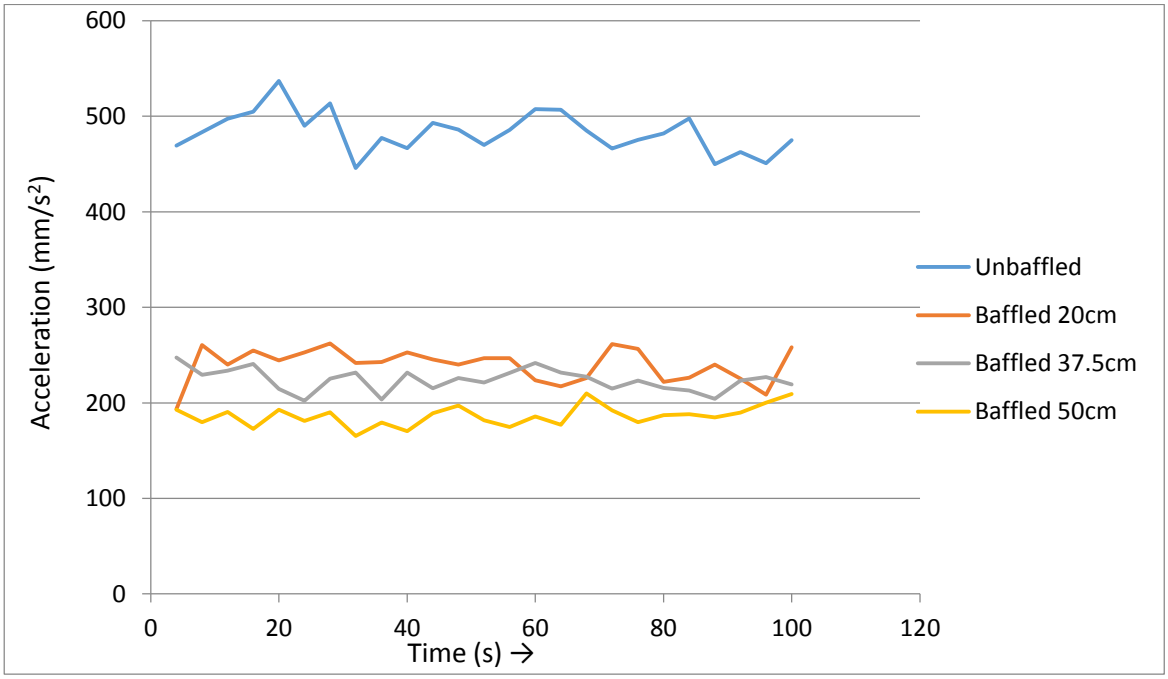

Fig 5.13 Comparison between acceleration for 75% fill for frequency 1.6 Hz

5.3.2.2 For 75% fill and frequency of 2.2 Hz

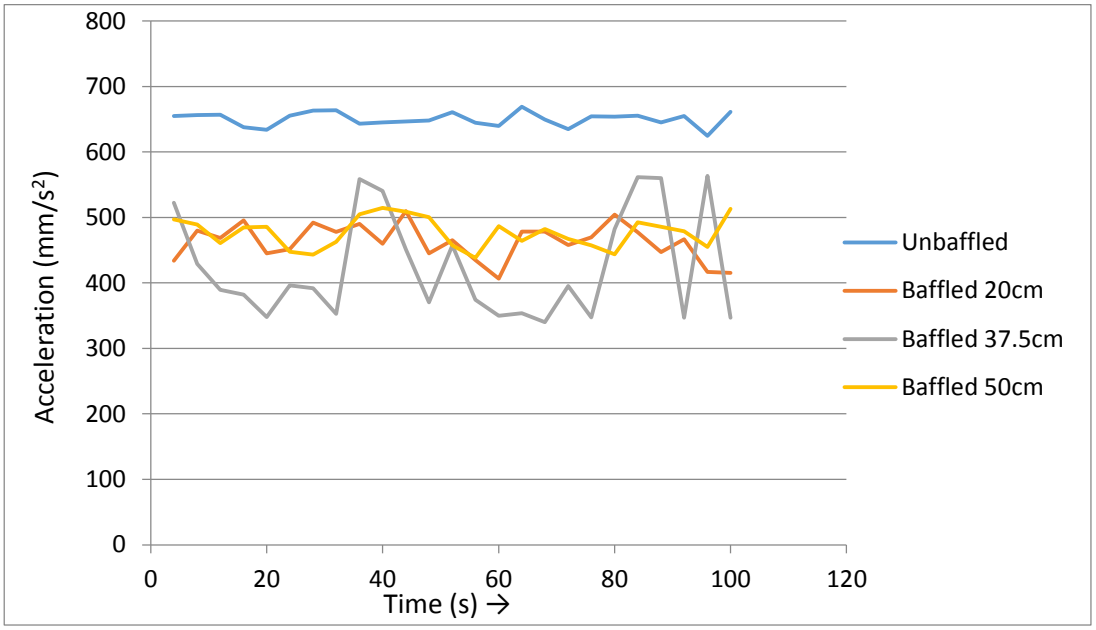

Fig 5.14 Comparison between acceleration for 75% fill for frequency 2.2 Hz

5.3.2.3 For 75% fill and frequency of 3.7 Hz

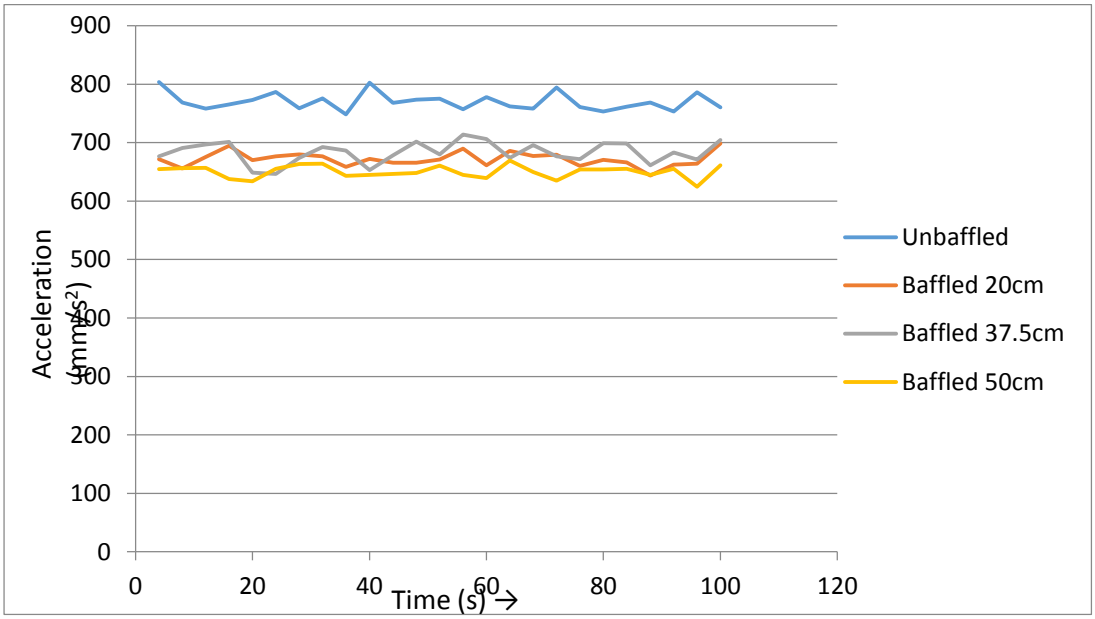

Fig 5.15 Comparison between acceleration for 75% fill for frequency 3.7 Hz

6.3.2.4 For 75% fill and frequency of 4.4 Hz

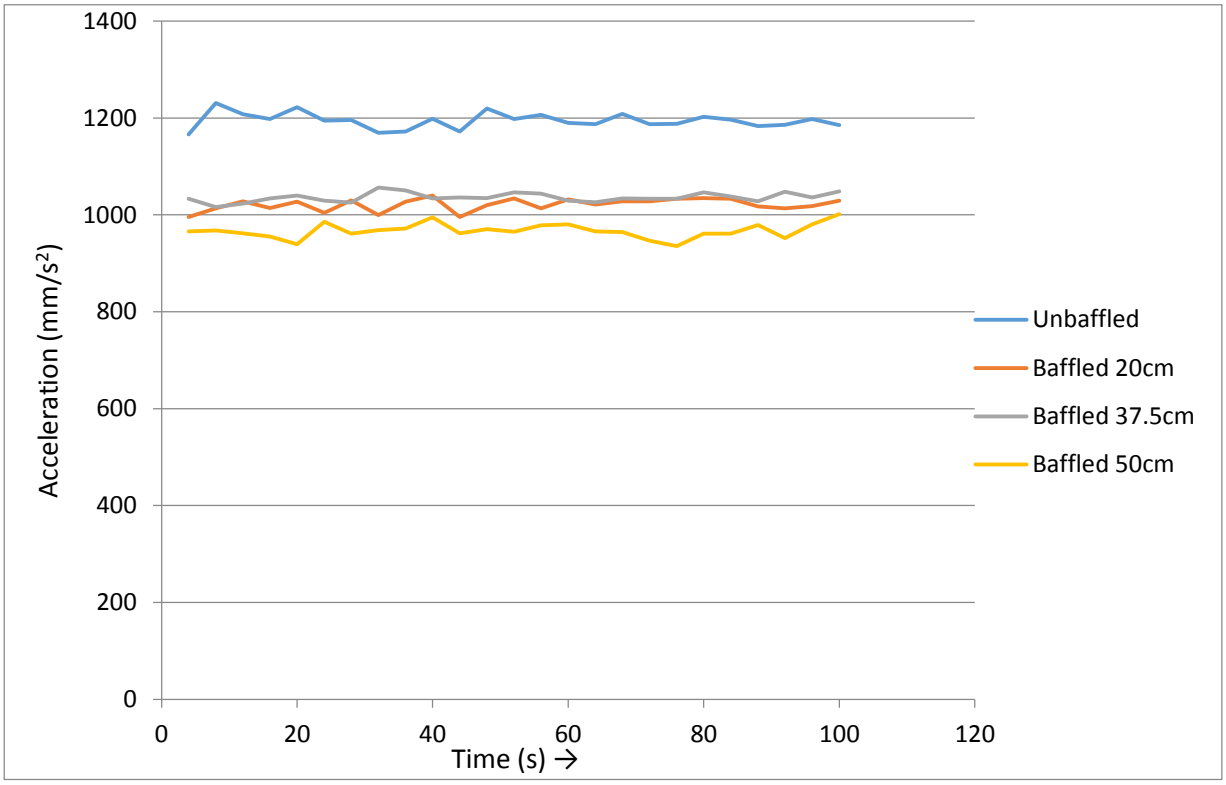

Fig 5.16 Comparison between acceleration for 75% fill for frequency 4.4 Hz

From the above graphs, it can be inferred that the value of acceleration for the unbaffled water tank is the maximum for all the cases of frequency.

Also, for most of the cases, as the height of baffle wall increases, the acceleration value decreases. That is, the value of acceleration for 20 cm long baffle wall is lesser than the unbaffled and further the value decreases for 37.5 cm and 50 cm long baffle wall.

The introduction of the baffles in the water tank decreases the sloshing effect by a considerable amount. In our experiment, introduction of baffle walls have reduced the average acceleration value by approximate 40%. This happens because the baffle walls dissipate the excess kinetic energy to the walls.

As the baffle wall height increases, the liquid sloshing becomes more suppressed due to the buildup of blockage effect of the baffle which results in additional viscosity and energy dissipation, also known as hydrodynamic damping.

5.4 Comparison between maximum acceleration as per change in frequency

5.4.1 For 50% fill water tank

5.4.1.1 Without baffle wall

Table 5.2 Variation between Maximum acceleration and frequency at 50% fill without baffle wall

Frequency (Hz)	Maximum Acceleration (mm/s^2)
1.6	601.6473
2.8	928.9089
3.7	1180.143
4.4	1254.254

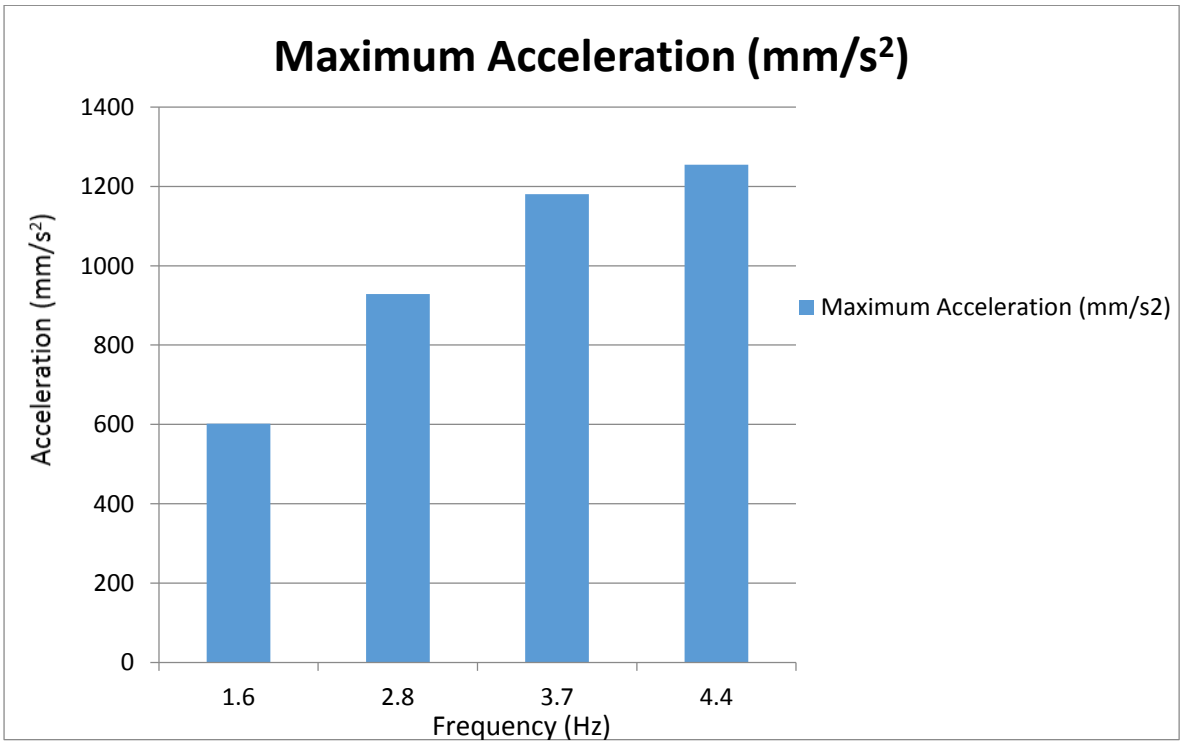

Fig 5.17 Variation between Maximum acceleration and frequency at 50% fill without baffle wall

5.4.1.2 With 12 cm baffle wall

Table 5.3 Variation between Maximum acceleration and frequency at 50% fill with 12 cm baffle wall

Frequency (Hz)	Maximum Acceleration (mm/s^2)
1.6	348.9417
2.8	785.0943
3.7	928.9089
4.4	1111.473

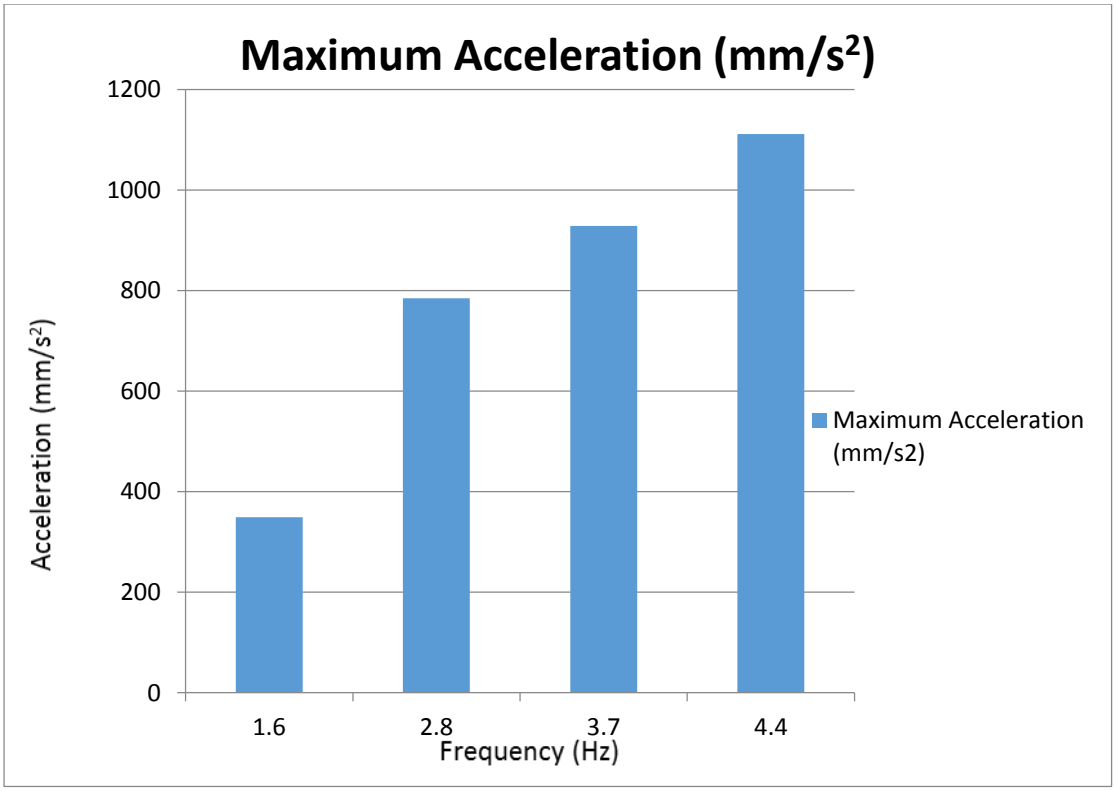

Fig 5.18 Variation between Maximum acceleration and frequency at 50% fill with 12 cm baffle wall

5.4.1.3. With 25 cm baffle wall

Table 5.4 Variation between Maximum acceleration and frequency at 50% fill with 25 cm baffle wall

Frequency (Hz)	Maximum Acceleration (mm/s^2)
1.6	359.7327
2.8	681.0102
3.7	731.9241
4.4	1071.252

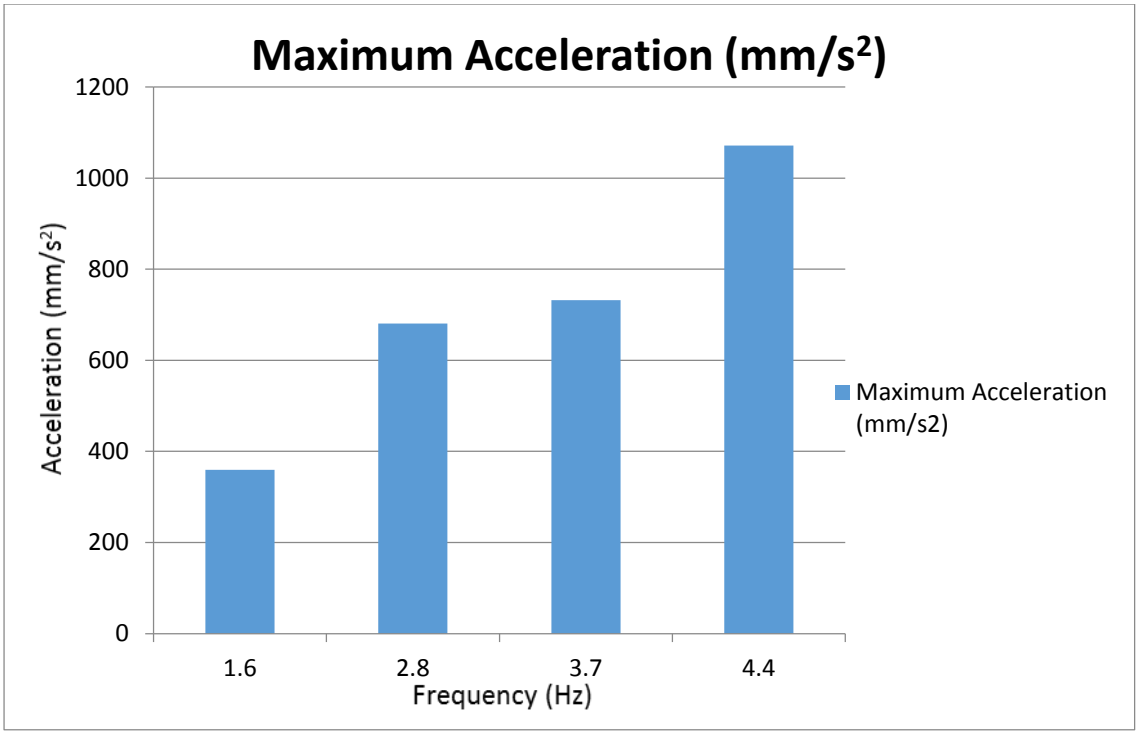

Fig 5.19 Variation between Maximum acceleration and frequency at 50% fill with 25 cm baffle wall

5.4.1.4. With 37 cm baffle wall

Table 5.5 Variation between Maximum acceleration and frequency at 50% fill with 37 cm baffle wall

Frequency (Hz)	Maximum Acceleration (mm/s^2)
1.6	260.6517
2.8	601.6473
3.7	604.254
4.4	1052.613

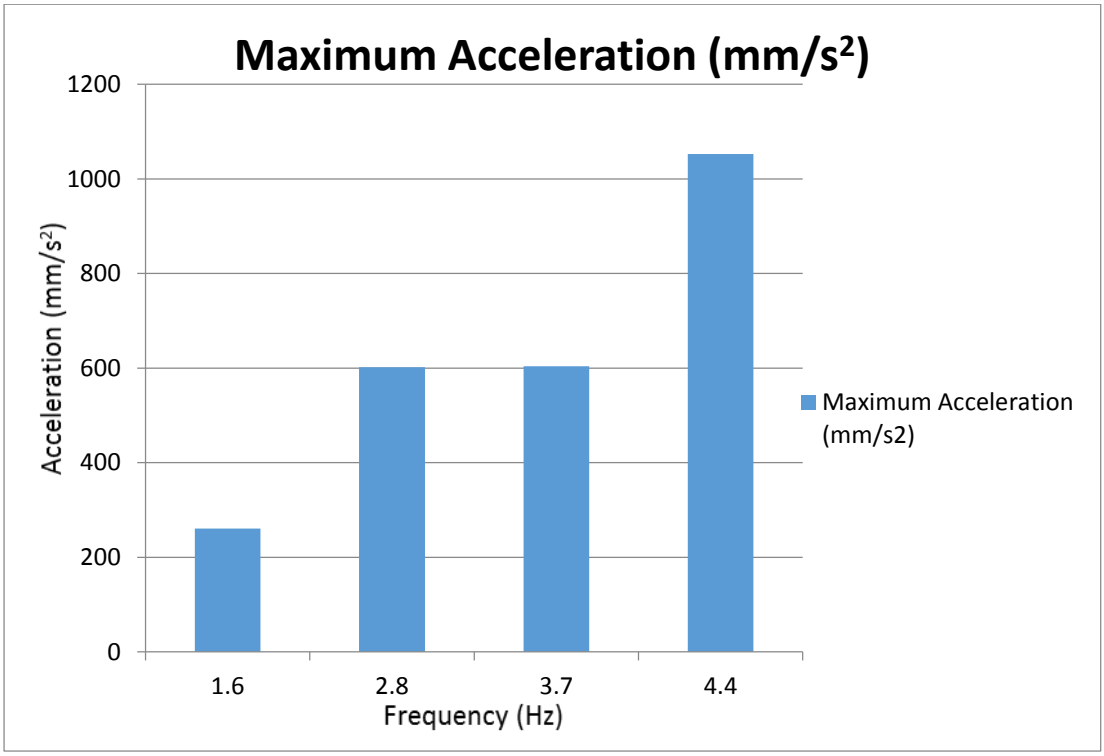

Fig 5.20 Variation between Maximum acceleration and frequency at 50% fill with 37 cm baffle wall

5.4.2 For 75% fill water tank

6.4.2.1 Without baffle wall

Table 5.6 Variation between Maximum acceleration and frequency at 75% fill without baffle wall

Frequency (Hz)	Maximum Acceleration (mm/s2)
1.6	536.9013
2.8	669.2382
3.7	803.439
4.4	1231.155

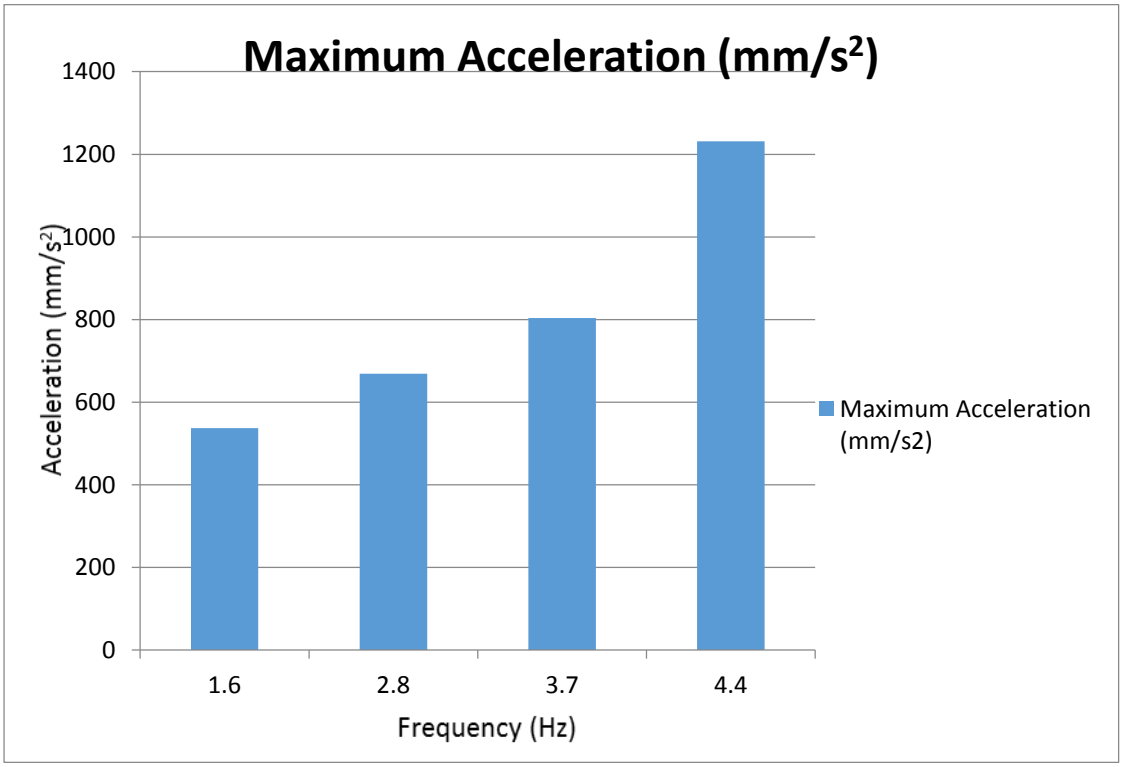

Fig 5.21 Variation between Maximum acceleration and frequency at 75% fill without baffle wall

5.4.2.2 With 20 cm baffle wall

Table 5.7 Variation between Maximum acceleration and frequency at 75% fill with 20 cm baffle wall

Frequency (Hz)	Maximum Acceleration (mm/s2)
1.6	262.1232
2.8	509.7276
3.7	698.2758
4.4	1039.86

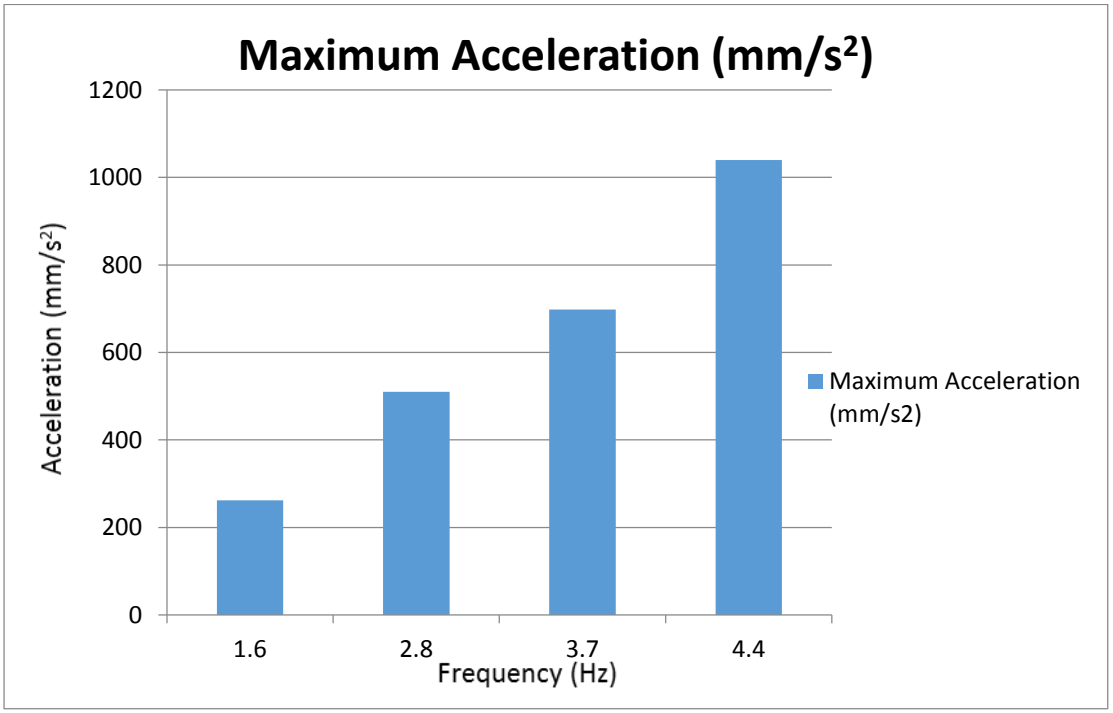

Fig 22Variation between Maximum acceleration and frequency at 75% fill with 20 cm baffle wall

5.4.2.3 With 37.5 cm baffle wall

Table 5.8 Variation between Maximum acceleration and frequency at 75% fill with 37.5 cm baffle wall

Frequency (Hz)	Maximum Acceleration (mm/s2)
1.6	247.5063
2.8	563.6826
3.7	713.9718
4.4	1056.537

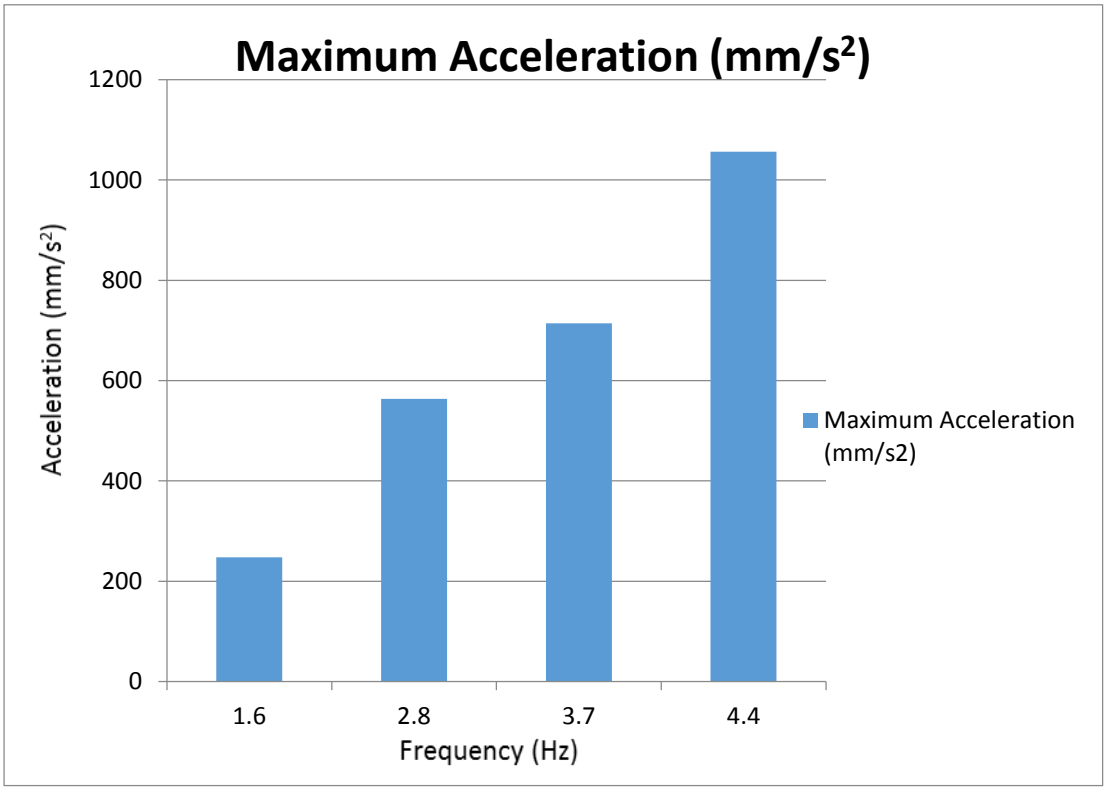

Fig 5.23 Variation between Maximum acceleration and frequency at 75% fill with 37.5 cm baffle wall

5.4.2.4 With 50 cm baffle wall

Table 5.9 Variation between Maximum acceleration and frequency at 75% fill with 50 cm baffle wall

Frequency (Hz)	Maximum Acceleration (mm/s2)
1.6	209.7378
2.8	514.7307
3.7	669.2382
4.4	1001.601

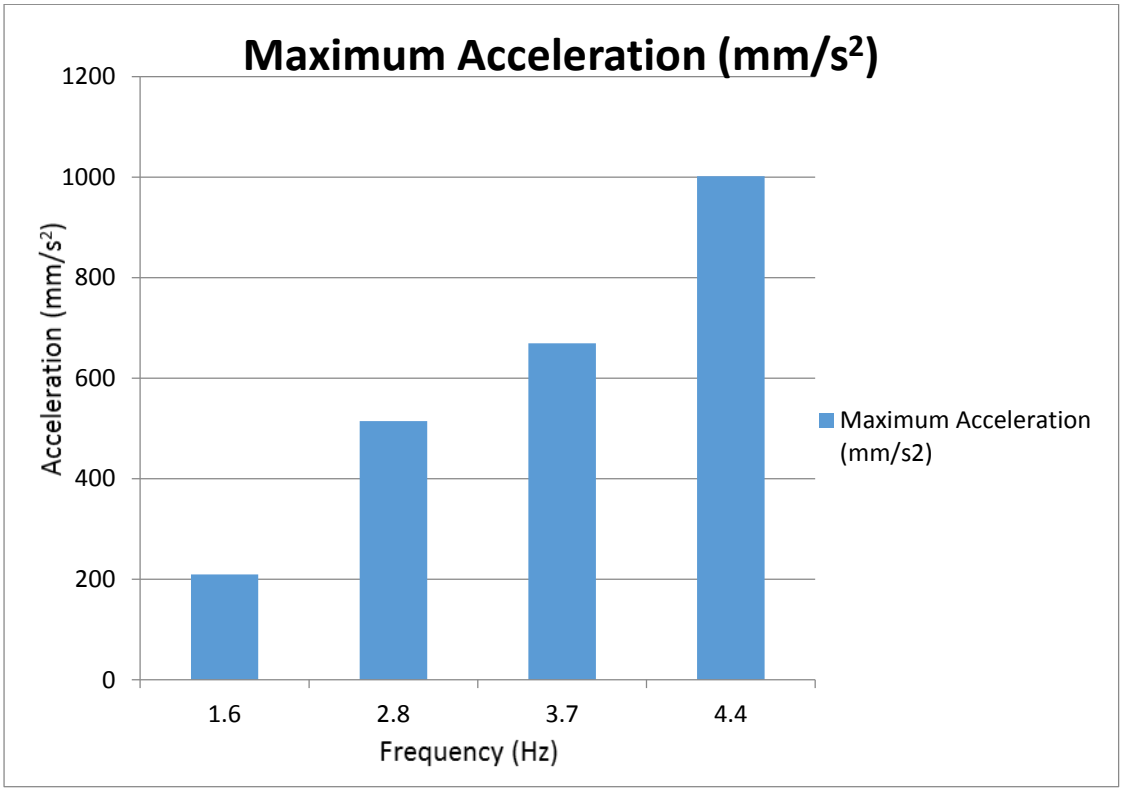

Fig 5.24 Variation between Maximum acceleration and frequency at 75% fill with 50 cm baffle wall

From all of the above graphs, it is clear that with the increase in frequency of excitation of the water tank, the maximum acceleration value increases. This is due to the reason that higher frequency imparts more energy to the water molecules which are transferred in the form of accelerations in the sensors attached with the water tank.

5.5 Comparison between accelerations as per change in type and configuration of baffle wall

5.5.1 Comparison between unbaffled tank, tank with 25 cm baffle wall and tank with perforated baffle wall at frequency of 2.8 Hz

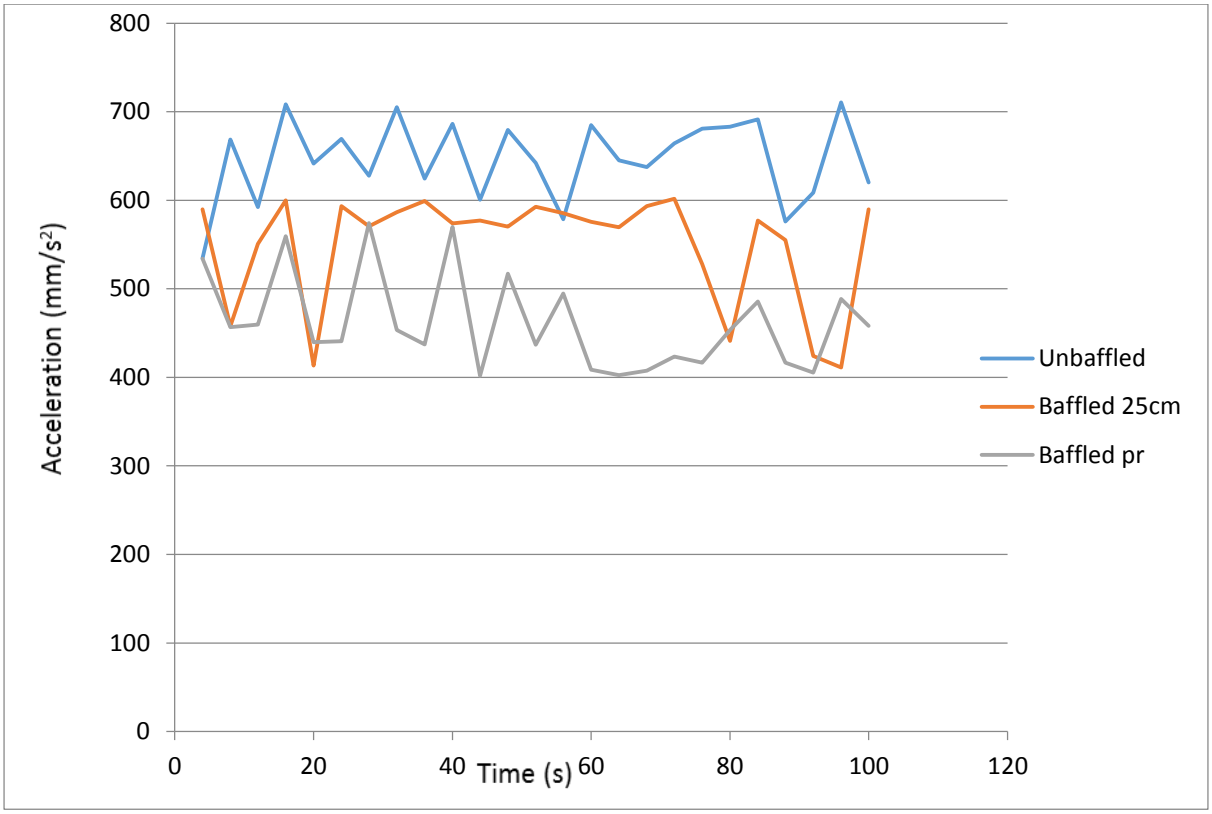

Fig 5.25 Comparison between unbaffled tank, tank with 25 cm baffle wall and tank with perforated baffle wall at frequency of 2.8 Hz

From the above graph, we can infer that after installation of the baffle wall the acceleration values are reduced up to 44% whereas when we used perforated type baffle wall, the accelerations were reduced up to 15%.

5.5.2 Comparison between accelerations when perforated baffle wall of type 1, type 2 and type 3 are used at frequency of 2.8 Hz

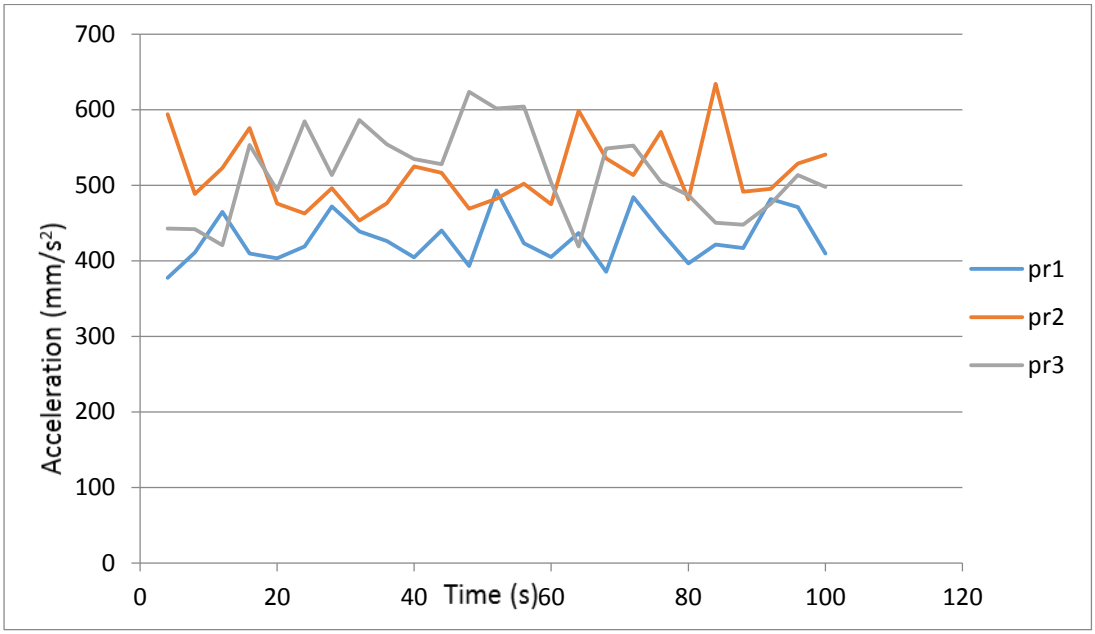

Fig 5.26Comparison between unbaffled tank, tank with 25 cm baffle wall and tank with perforated baffle wall at frequency of 2.8 Hz

From this graph, it can be inferred that perforated baffle wall type 1 is the safest in reducing the sloshing effect followed by type 2 and type 3.

5.5.3 Comparison between unbaffled tank, tank with 25 cm baffle wall and tank with perforated baffle wall at frequency of 3.7 Hz

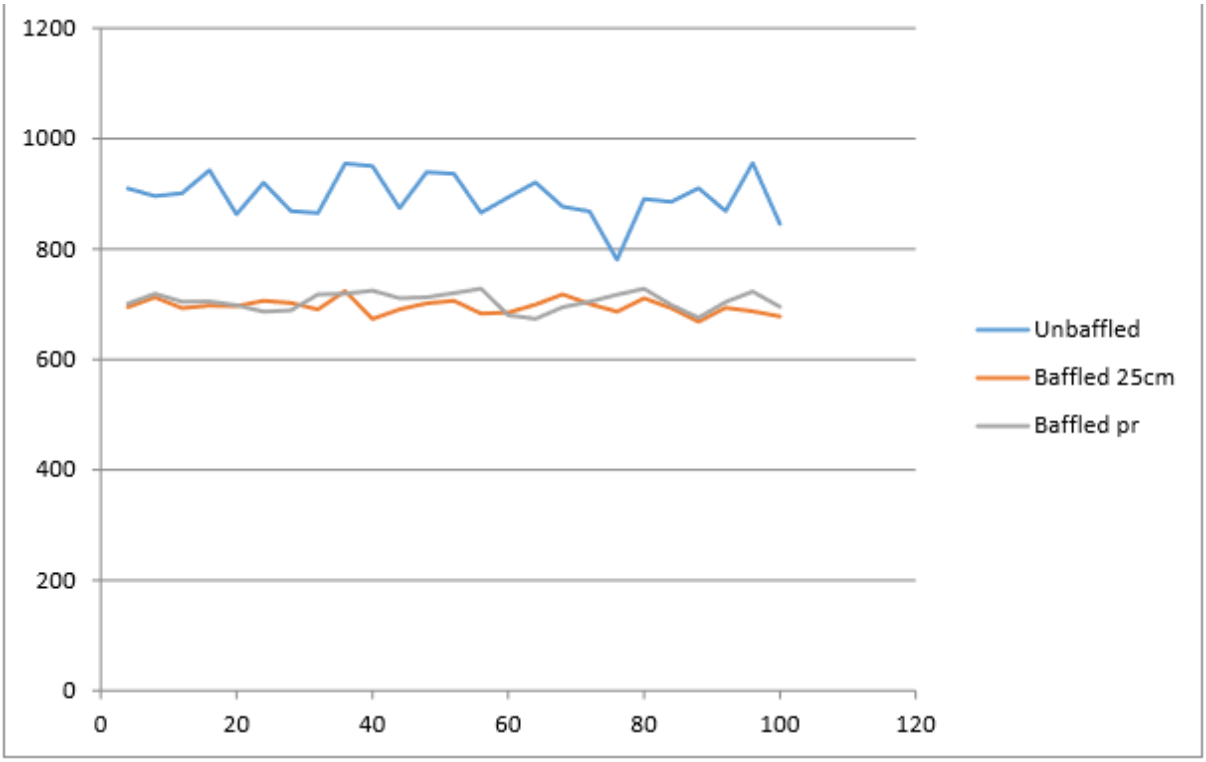

Fig 5.27 Comparison between unbaffled tank, tank with 25 cm baffle wall and tank with perforated baffle wall at frequency of 3.7 Hz

From this graph, we can infer that after installation of baffle wall, both baffle walls showed nearly the same behaviour and the sloshing effect was reduced by 25 %.

5.5.4 Comparison between accelerations when perforated baffle wall of type 1, type 2 and type 3 are used at frequency of 3.7 Hz

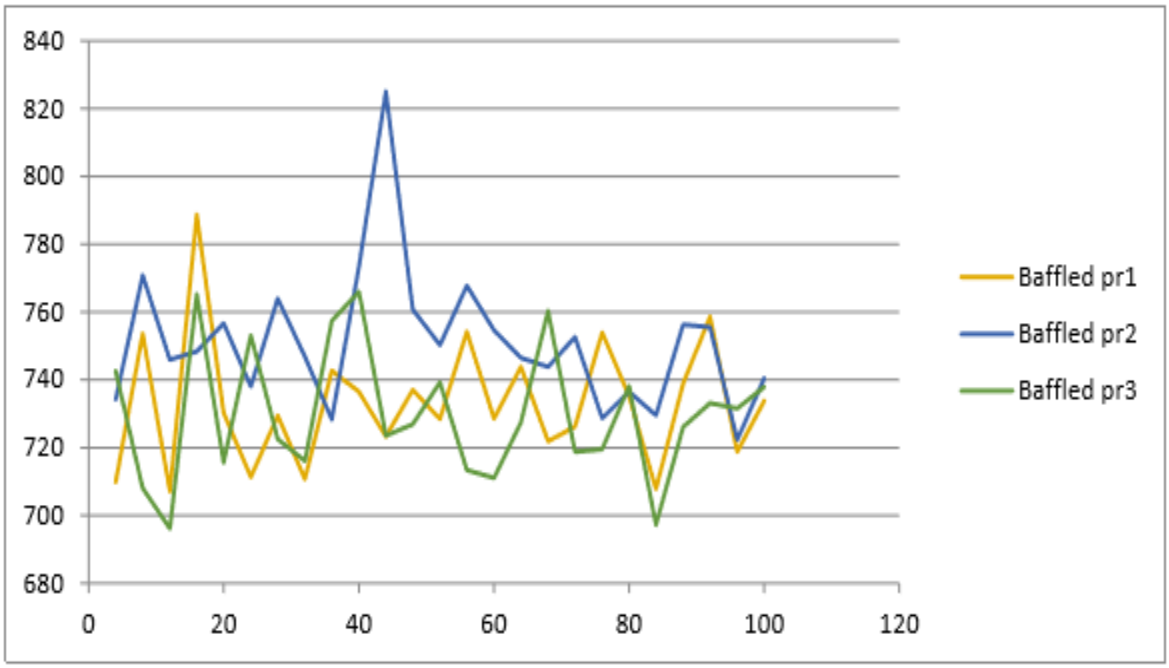

Fig 5.28 Comparison between unbaffled tank, tank with 25 cm baffle wall and tank with perforated baffle wall at frequency of 3.7 Hz

In the above graph, large variations are observed for accelerations for type 1, 2 and 3 baffle wall. This could be arising due to experimental error or due to error arising due to improper fixation of accelerometers

CHAPTER 6
CONCLUSIONS

6.1 Conclusions

1. The acceleration value increases in magnitude with the increase in height of position of accelerometer from bottom

2. The introduction of the baffles in the water tank decreases the sloshing effect by a considerable amount. In our experiment, introduction of baffle walls have reduced the average acceleration value by approximate 40%. This happens because the baffle walls dissipate the excess kinetic energy to the walls.

3. As the baffle wall height increases, the liquid sloshing becomes more suppressed due to the build-up of blockage effect of the baffle which results in additional viscosity and energy dissipation.

4. With the increase in frequency of excitation of the water tank, the maximum acceleration value increases.

5. The maximum free surface displacement of the liquid in the tank, for a particular excitation frequency, rises the most when the tank is least filled. This is due to the self-damping property of the liquid.

6. After installation of the baffle wall the acceleration values are reduced up to 44% whereas when we used perforated type baffle wall, the accelerations were reduced up to 15%.

7. From this graph, it can be inferred that perforated baffle wall type 1 is the most safe in reducing the sloshing effect followed by type 2 and type 3.

6.2 Scope for future study

Following can be the scope for the future research study:

1.Different other configurations of baffles can be analysed to optimize the design of the tank to further reduce the sloshing phenomenon.

2. The dimensions of the baffles can also be optimized for further reduction in the sloshing. Sloshing under more seismic excitation amplitude can also be investigated.

3 Effect of spacing of walls and thickness of baffle walls can also be studied.

4.Multiple baffle walls and upper mounted baffle walls can be used to study the reduction in sloshing.

References

1. Isaacson, M., Premasiri, S., 2001. Hydrodynamic damping due to baffles in a rectangular tank. Can. J. Civ. Eng. 28 (4), 608–616.

2. Akyildiz, H., Unal, E., 2005. Experimental investigation of pressure distribution on a rectangular tank due to the liquid sloshing. Ocean Eng. 32, 1503–1516.

3. Cho, J.R., Lee, H.W., 2004. Numerical study on liquid sloshing in baffled tank by nonlinear finite element method. Comput. Methods Appl. Mech. Eng. 193 (23–26), 2581–2598.

4. Younes, M.F., Younes, Y.K., El-Madah, M., Ibrahim, I.M., El-Dannanh, E.H., 2007. An experimental investigation of hydrodynamic damping due to vertical baffle arrangements in a rectangular tank. In: Proceedings of the Institution of Mechanical Engineers, Part M: Journal of Engineering for the Maritime Environment, vol. 221, pp. 115–123.

5. Liu, D., Lin, P., 2009. A numerical study of three-dimensional liquid sloshing in tanks. Ocean Eng. 36, 202–212.

6. Panigrahy, P.K., Saha, U.K., Maity, D., 2009. Experimental studies on sloshing behavior due to horizontal movement of liquids in baffled tanks. Ocean Eng. 36, 213–222.

7. Serdar Celebi, M., Akyildiz hakan (2002) "Nonlinear modeling of liquid sloshing in moving rectangular tank", Ocean Engineering 29,1527-1553.

8. Mohammed Ali Goudarzi and Saeed Reza Sabbagh Yaazdi (2012) "Investigation of nonlinear sloshing effects in seismically excited tank", Soil Dynamics and Earthquake Engineering 43,355-365.

9. Heng Jin, Yong Liun, Hua-Jun Li (2014) "Experimental study on sloshing in a tank with an inner horizontal perforated plate" , Ocean Engineering 82 (2014) 75–84.

10. Bernard Molinn, Fabien Remy (2013) " Experimental and numerical study of the sloshing motion in a rectangular tank with a perforated screen", Journal of Fluids and Structures 43 (2013) 463–480.

11. Development of experimental setups for earthquake engineering education National Program on Earthquake Engineering Education, MHRD, Government of India C S Manohar and S Venkatesha (April 2006)